CCI

BIOMASS

ALGORITHM DEVELOPMENT PLAN

VERSION 5.0

DOCUMENT REF:	CCI_BIOMASS_ADP_V5
DELIVERABLE REF:	D2.4-ADP
VERSION:	5.0
CREATION DATE:	2021-06-16
LAST MODIFIED	2023-12-12

Document Authorship

	NAME	FUNCTION	ORGANISATION	SIGNATURE	DATE
PREPARED	M. Santoro	Project scientist	Gamma Remote Sensing		
PREPARED	O. Cartus	Project scientist	Gamma Remote Sensing		
PREPARED	H. Balzter	WP Lead	University of Leicester		
PREPARED	N. Acil	Project scientist	University of Leicester		
PREPARED	R. Lucas	Project manager	Aberystwyth University		
PREPARED					
PREPARED					
PREPARED					
PREPARED					
VERIFIED	H. Friendship-Kay	Project Coordinator	Aberystwyth University		
VERIFIED	S. Quegan	Science Leader	Sheffield University		
APPROVED					

Document Distribution

ORGANISATION	NAME	QUANTITY
ESA	Frank Seifert	

Document History

VERSION	DATE	DESCRIPTION	APPROVED
1.0	2019-03-05	ADP of CCI Biomass year 1	
2.0	2020-04-06	ADP of CCI Biomass year 2	
3.0	2021-06-16	ADP of CCI Biomass year 3	
4.0	2023-02-09	ADP of CCI Biomass year 4	
5.0	2023-12-12	ADP of CCI Biomass year 4	

Document Change Record (from Year 1 to Year N)

VERSION	DATE	DESCRIPTION	APPROVED
2.0	2020-04-06	Adapted the ADP to year 2 algorithm. Added the strategy to map AGB changes	
3.0	2021-06-16	Adapted the ADP to year 3 algorithm. Added aspects to be developed in future studies	

4.0	2023-03-30	Adapted the ADP to year 4 algorithm. Added aspects to be developed in future studies	
5.0	2023-12-12	Adapted the ADP to year 5 algorithm. Added aspects developed on biomass change.	

TABLE OF CONTENTS

LIST OF FIGURES

SYMBOLS AND ACRONYMS

ADP	Algorithm Development Plan
AGB	Above Ground Biomass
AFOLU	Agriculture, Forestry and Other Land Use
ALOS	Advanced Land Observing Satellite
ARD	Analysis Ready Data
ASCAT	Advanced Scatterometer
ATBD	Algorithm Theoretical Basis Document
BCEF	Biomass Conversion & Expansion Factor
CCI	Climate Change Initiative
CCI-Biomass	Climate Change Initiative – Biomass
CTV	Cultivated Terrestrial Vegetation
DARD	Data Access Requirements Document
E3UB	End to End ECV Uncertainty Budget
ECV	Essential Climate Variables
EO	Earth Observation
ESA	European Space Agency
FAO	Food and Agriculture Organisation
GCOS	Global Climate Observing System
GEDI	Global Ecosystem Dynamics Investigation
GEE	Google Earth Engine
GHGs	Greenhouse Gases
GLAS	Geoscience Laser Altimeter System
GSV	Growing Stock Volume
ICESat	Ice, Cloud, and land Elevation Satellite
JAXA	Japan Aerospace Exploration Agency
LCCS	Land Cover Classification System
NDVI	Normalised Difference Vegetation Index
NFI	National Forest Inventory
NTV	Natural/Semi-Natural Terrestrial Vegetation
OED	Overarching Environmental Descriptor
PSD	Product Specification Document
PVASR	Product Validation and Algorithm Selection Report
PVIR	Product Validation and Intercomparison Report
PVP	Product Validation Plan
SAR	Synthetic Aperture Radar

SMAP	Soil Moisture Active Passive
SMOS	Soil Moisture & Ocean Salinity
SRTM	Shuttle Radar Topography Mission
URD	User Requirement Document
WCM	Water Cloud Model

Table 1-1: Reference Documents

ID	TITLE	ISSUE	DATE
RD-1	Users Requirements Document		
RD-2	Product Specification Document		
RD-3	Data Access Requirements Document		
RD-4	Product Validation and Algorithm Selection		
RD-5	Algorithm Theoretical Basis Document		
RD-6	End to End ECV Uncertainty Budget		
RD-7	Product Validation Plan		
RD-8	Algorithm Theoretical Basis Document of GlobBiomass project		
RD-8	Product Validation and Intercomparison Report		

1. Introduction

Above-ground biomass (AGB, units: Mg ha^{-1}) is defined by the Global Carbon Observing System (GCOS) as one of 54 Essential Climate Variables (ECV). For climate science communities, AGB is a pivotal variable of the Earth System, as it impacts the surface energy budget, the land surface water balance, the atmospheric concentration of greenhouse gases (GHGs) and a range of ecosystem services. The GCOS requirement is for AGB to be provided wall-to-wall over the entire globe for all major woody biomes at 500 m to 1 km spatial resolution with a relative error of less than 20% where AGB exceeds 50 Mg ha^{-1} and a fixed error of 10 Mg ha^{-1} where the AGB is below that limit.

One of the objectives of the Climate Change Initiative (CCI) Biomass project is to generate global maps of AGB using a variety of Earth Observation (EO) datasets and state-of-the-art models for several epochs and assess AGB changes over 1-year differences and a 10-year difference. The maps should be thematically consistent with data layers similar to the AGB datasets that are produced in the framework of the CCI Programme (e.g., Fire, Land Cover, Snow etc.).

Algorithms to estimate AGB from EO data are described in the Algorithm Theoretical Basis Document (ATBD) [RD-5] while the End-to-End ECV Uncertainty Budget (E3UB) document [RD-6] describes the precision associated with the estimates of AGB and AGB change. The ATBD and the E3UB documents are live documents, updated annually to provide a thorough description of the algorithms implemented to generate AGB and AGB change maps. The current version of the ATBD and the E3UB documents describe the CORE algorithm used to generate version 5 of the Climate Research Data Package. This consists of global datasets of AGB and related AGB change maps using data representative for the years 2010 and between 2015 and 2021.

1.1. Background to this document

The original CORE algorithm was based on the GlobBiomass global retrieval algorithm [RD-8] (see http://globbiomass.org/products/global-mapping/).

For version 2, the CORE algorithm was enhanced by expanding on concepts presented in the first version of this document. Namely, (i) the retrieval models expressed the Synthetic Aperture Radar (SAR) backscatter as a function of forest height and canopy density, (ii) models between canopy density, forest height and AGB were implemented in the retrieval models (iii) the model training accounted for the effect of local topography on the relationship between SAR backscatter and biomass. These advances were possible thanks to an in-depth analysis of the Ice, Cloud and land Elevation Satellite (ICESat) Geoscience Laser Altimeter System (GLAS) observations of canopy density and height (Kay et al., 2021), and the increasing number of publications that focus on the relationship between LiDAR height metrics and AGB. As a consequence, the CORE retrieval algorithm provided estimates of AGB instead of Growing Stock Volume (GSV) so that a Biomass Conversion and Expansion Factors (BCEF) layer becomes unnecessary.

For version 3, the CORE algorithm was consolidated with the addition of recent LiDAR observations by the Global Ecosystem Dynamics Investigation (GEDI) and the ICESat-2 missions. Also, the CORE algorithm implemented measures to avoid unnatural fluctuations of the AGB estimates. These measures, however, could not fully compensate for artefacts because of the different setting of the EO data available in 2010, 2017 and 2018. To quantify biases in each of the three maps, a model-based framework relying on the plot database available to CCI Biomass was implemented with the Plot2Map tool (Araza et al., 2022) and coarse resolution maps of AGB bias (0.1°) were generated. The bias layers are supposed to build confidence on the reliability of the map rather than to represent a correction factor to be applied straight to the AGB estimates, also because of the much poorer pixel spacing (10,000 ha vs. 1 ha). The AGB change maps derived from the Year 3 dataset were based on AGB differencing rather than signal differencing because of the multi-sensor approach pursued in this project. Given that AGB changes were assessed on maps of different quality and only for three epochs, the approach was preliminary.

For version 4, the estimation of AGB relied on annual multi-temporal observations of L-band SAR backscatter, which replaced the annual mosaics (i.e., a single observation) and on more extensive datasets from spaceborne LiDAR missions. LiDAR data, together with a large database of AGB statistics published by National Forest Inventories (NFIs), allowed a more accurate characterisation of the model that expresses height as a function of AGB. With such a model, systematic retrieval errors, due for example to an incorrect characterisation of the maximum AGB in a region, could be alleviated. Indeed, we identified this parameter as causing significant biases and thus being a major issue in previous versions of the Climate Research Data Package (CRDP). The retrieval models based on the BIOMASAR approach evolved towards a more precise characterisation of the parameters in the Water Cloud Model (WCM) relating AGB to SAR backscatter. The retrieval was also relaxed in regions with sloping terrain because the SAR data had higher radiometric quality than in previous project years. In addition, the merging rules for BIOMASAR-C and -L AGB were revisited to better account for their mutual contribution. The availability of a time series of AGB estimates from each of the approaches allowed for more robust merging rules to be defined.

The estimation of AGB change has not departed from its original formulation, i.e., a map differencing approach. The assessment of AGB change maps based on AGB differences with a time series of maps created with state-of-art retrieval techniques was the overall objective of algorithmic advances in the AGB change mapping for version 4.

For the current version, the estimation of AGB has been consolidated. Multi-temporal SAR acquisitions are now available throughout the entire interval foreseen for AGB mapping. Also the spaceborne LiDAR dataset has been populated with more recent measurements to increase the spatial density. Validation of the CRDP v4 confirmed that the maximum AGB, i.e., the estimates of local maximum canopy height and the height-to-AGB model, have great impact on the level of the AGB estimates. For this version, the fit of this model has been revised. We also approached several aspects pointed at in the previous version of this document, namely, the retrieval errors due to banding, topography and stratification by vegetation type. While the first two cannot be corrected for because caused by artefacts in the original SAR datasets, a mangrove-specific model training was introduced for this version. AGB change still relies on the differencing method. In this version of the ADP, we illustrate several approaches that diagnose the reliability of the differencing method.

1.2. Content of this document

Some ideas to be pursued in future activities are presented in this document. Such ideas involve both the estimation of AGB and the estimation of AGB over time to track changes, as it is believed that a multi-sensor approach to estimating AGB is superior to using a single set of observations. With the multi-sensorial approach, it is not possible to relate a change in AGB to a change in signals.

This document builds on the ATBD and E3UB documents for v5 to identify major elements that require development in future years of the CCI Biomass project. In addition, we consider the review of the CCI BIOMASS data products of v4 reported in the Product Validation and Intercomparison Report (PVIR) [RD-8]. As for the ATBD and the E3UB documents, this Algorithm Development Plan relies on the most recent versions of the Users Requirements Document (URD) [RD-1] and the Product Specifications Document (PSD) [RD-2].

Section 2 reviews the CCI Biomass CORE algorithm implemented in v5. Section 3 elaborates on the known major weaknesses of the CORE algorithm based on the initial assessment of AGB retrieval reported in the ATBD. Section 4 lists potential solutions to the issues identified in Section 3. Advancing the estimation of AGB change based on the experiences gathered with the AGB data products foreseen by the CRDP of the CCI Biomass project is the topic of Section 5.

2. CCI Biomass CORE algorithm

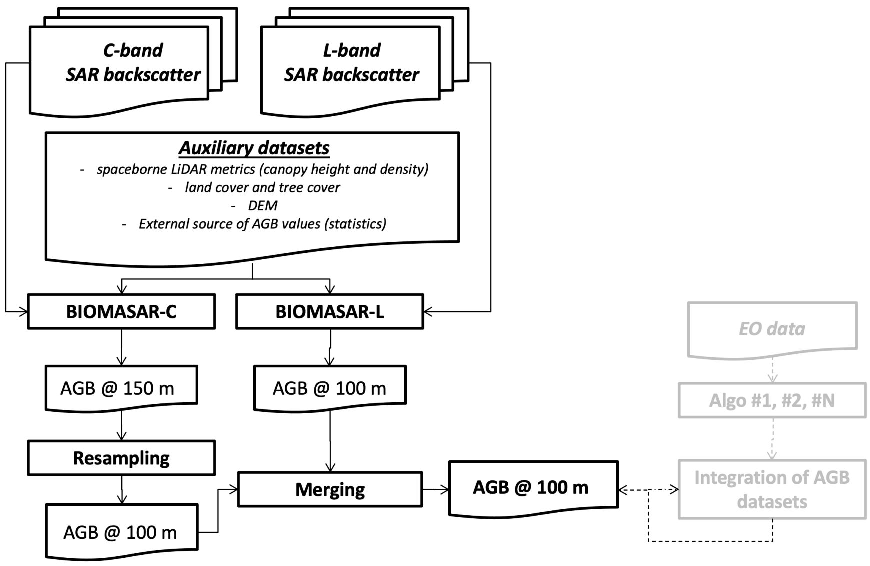

Figure 2-1: Functional dependencies of datasets and approaches forming the CCI Biomass CORE global biomass retrieval algorithm. The shaded part of the flowchart represents potential improvements following the implementation of additional retrieval techniques [RD-3].

Figure 2-1 shows the flowchart of the CORE biomass estimation procedure of the CCI Biomass project to generate annual, global datasets of AGB estimates [RD-5]. The shaded part of the flowchart represents potential improvements following the implementation of additional retrieval techniques. [RD-5].

With the CORE algorithm, two independent estimates of AGB are obtained from the same BIOMASAR algorithms but with different modelling frameworks. The SAR backscatter is related to canopy density and height with a WCM, i.e., a parametric model that simplifies the scattering in the canopy and below the canopy with a few parameters and variables (canopy density and canopy height). A simple model, trained with LiDAR data, is used to relate these variables. A second model, linking height and AGB, is then used to express the SAR backscatter directly as a function of AGB. Linear weighting of AGB estimates obtained from the inversion of the WCM and single backscatter observations is applied to generate a final estimate of AGB.

In v5, the SAR datasets consisted of the best possible setting of (freely available and global) images. The Sentinel-1 dataset has been consolidated in the form of monthly averages to speed up computation and reduce redundancies. The Advanced Land Observing Satellites (ALOS) -1 and -2 SAR datasets have been provided by the Japanese Aerospace Exploration Agency (JAXA) in the form of individual strips for the Fine Beam mode and per-cycle mosaics of 46 days for the ScanSAR mode. Each location is now characterised by multiple dual-polarised observations as opposed to a single dual-pol observation from the annual mosaics used until v3.

Following the approach that was started in Year 3, the CORE algorithm makes even more explicit use of laser observations in the retrieval model and follows a promising line of research aiming at relating LiDAR-based canopy height metrics to AGB measurements rather than to AGB estimates from maps. Also, the retrieval still accounts for topography by using experimental relationships between incidence angle and the SAR backscatter rather than developing models that would have probably failed due to the subtle difference in backscatter as landscape and topography change. Finally, the estimation of the model parameters implements a robust model calibration approach consisting of a blend of self-calibration and least squares regression with respect to a reference dataset of canopy density. Merging of AGB estimates from BIOMASAR-C and BIOMASAR-L now exploits the time series of AGB estimates from each approach to construct a set of merging rules of increased robustness with respect to the weights used in previous versions of the CRDP. Quantitative assessment of the results achieved with the CORE algorithm is presented in the PVIR.

3. Caveats of the CORE algorithm

The above brief summary of the CCI Biomass CORE algorithm highlights the major elements of the retrieval approach. This may not be the best possible algorithm but rather is a global approach constrained by the available EO data and ground observations. The CCI Biomass CORE algorithm relies on several assumptions that appear viable when comparing large-scale averages of estimated AGB with corresponding values based on inventory information [RD-5] and [RD-7]. Nevertheless, these assumptions, which were made to allow the CORE algorithm to perform globally, also introduce systematic errors into the retrieved AGB, which may become apparent when focusing on particular areas [RD-4], [RD-5] and [RD-7].

Here, we provide a list of caveats and potential areas of improvement of the CORE algorithm. These are then expanded in Section 4 with a proposed development of the CORE algorithm.

- The retrieval of AGB implemented in v1 was found to be rather conservative because it missed the extreme values of AGB. One of the reasons was that the retrieval models were canopy-centric and did not explicitly involve height information. In v2, we exploited height information in the form of models, with interesting preliminary results. The models were based on ICESat GLAS metrics, which did not provide a uniform sampling of all land masses on Earth and required us to be rather generic in the way the models could describe the relationship between canopy density, height and AGB. With the denser coverage of GEDI and ICESat-2, the models between AGB and tree height were further characterized in v3. The impact of the models on the AGB maps was substantial, reducing the overestimation in the low AGB range and underestimation in the high AGB range. Both GEDI and ICESat-2 data products were still under development, which led to moderate usage in v3. In v4, the interaction with the data production teams and progressive ingestion of new data releases improved the models and, thereof, the auxiliary datasets used by the retrieval algorithms (e.g., the maximum AGB). The data were further investigated in v5 to understand the impact of errors on the map products and additional filters were implemented to prevent that macroscopic errors would generate biases. These investigations need to be pursued in the future as well with newer versions of the LiDAR data products being released.

- The AGB retrieval model uses two sets of models to link the SAR backscatter (predictor) to the response variable (AGB). These are under continual development as more data suitable for training the allometric models become available.
    - The model that expresses canopy density as a function of canopy height is based on LiDAR observations. As of v5, the CORE retrieval algorithm still implements the model trained on ICESat GLAS data. The GLAS dataset is strongly filtered to ensure a correct estimation of allometric parameters based on LiDAR data. The consequence is an uneven characterisation of these parameters because the density of the footprints was highly variable. GEDI data are the only alternative because both canopy density and canopy height are provided as part of the Level 2 datasets, whereas the ATL08 product based on ICESat-2 data only contains canopy height. Investigation of the relationship between canopy height and canopy density observations by GEDI revealed inconsistencies in the observations of canopy cover, which requires further investigations. The major limitation of a model based on GEDI data is the impossibility to characterise it throughout the boreal zone because of the coverage of GEDI is limited to latitudes between +/- 52°. To overcome this issue, measures need to be sought that harmonise models from ICESat GLAS and GEDI. Even though the data from the two missions were acquired during two different decades, we assume that the model is time-invariant.
    - The model that expresses canopy height as a function of AGB was based on spaceborne LiDAR observations and estimates of AGB from a map until v3. Several measures were implemented to limit the impact of the uncertainties affecting the map-based values of AGB on the model. Still, if any systematic error in the form of a bias affected the AGB estimates, these propagated to the estimates of the coefficients of the allometric function. For v4 and v5, we used a more extensive set of LiDAR observations than in previous versions of the CORE retrieval algorithm and attempted a new pathway to characterise the model by relying on AGB observations rather than on AGB estimates. The AGB observations consisted of average values reported by NFIs

at the level of administrative or ecological units and were related to average values of canopy height from spaceborne LiDAR data for the same units. To characterise the model in space, the data were grouped into regions. This approach was found to be promising. While the refinement of the regions improved the overall characterization of the model globally, we still identify several caveats that need to be addressed in future versions of the CORE retrieval approach. The NFI statistics are not harmonised with respect to each other, and the definition of forest land underlying the average values reported by the NFIs and used here to select the LiDAR footprints is not harmonised. The strata used to group observations were based on some macro-ecological patterns, which cancels out small scale variability of the relationship between height and AGB, for example due to spatial variability of wood density or growth factors. In addition, the use of average values instead of the original ones measured at plots and footprints might alter the shape of the model, leading to over- or under-estimates in the retrieved AGB. This aspect is difficult to approach because the NFI data used to generate the AGB statistics are not publicly available.

- The retrieval of AGB is based on some simplifying assumptions that cause the retrieval models to be too general to capture the spatial variability of the relationship between the radar observations and vegetation properties. Vegetation structural information should provide the backbone for a more targeted estimation of model parameters. Unfortunately, most EO-based datasets that could complement a retrieval do not have a full error characterisation so that the impact of a direct implementation in our retrieval schemes may not be controllable.

- Regarding alternative approaches to retrieving AGB from the set of observations currently available from spaceborne sensors, we have not identified any ground-breaking approaches that may improve our retrievals while at the same time fulfilling the requirements in terms of spatial resolution, temporal coverage and global representation of the CCI biomass maps. Non-parametric approaches based on machine learning or artificial intelligence are not targeted because they would not be supported by a dense and large range of AGB observations.

- A wide range of observations is, in our opinion, fundamental to avoid systematic biases caused by the fact that no remote sensing observation is a direct measure of biomass. One line of research that has been developing quickly in recent years is inversion of coarse-resolution observations from spaceborne microwave radiometers and scatterometers to AGB. Although such observations do not match the requirement on spatial resolution of the CCI Biomass maps, data from radiometer and scatterometer missions cover several decades and have been demonstrated to allow characterisation of biomass dynamics. As such, experiences gathered at coarse resolution may act as guidelines in the process of establishing rules to ensure that the dynamics of AGB obtained from less frequent high-resolution EO data are well captured.

- Finally, regardless of the procedures here developed to estimate AGB, the accuracy of the retrieval depends strongly on the quality of the EO data used as predictors. We have identified a number of systematic issues in the SAR data that prevent us obtaining the highest possible quality AGB results. It is believed that having the possibility to pre-process the EO data would allow such quality to be attained. Hence continual interaction with data providers is needed.

4. Proposed development of CORE algorithm

4.1. Consolidate the use of spaceborne LiDAR observations

Observations that sense forest structure are of major benefit to the estimation of AGB. Unfortunately, the majority of EO data available globally is in the form of energy reflected to the sensor, so that AGB can only be inferred with parametric or non-parametric approaches (Santoro and Cartus, 2018). SAR interferometry and laser scanning instead generate observations that contain information on the vertical and horizontal distribution of vegetation, thus providing a more direct measure of parameters involved in the computation of biomass (canopy height, density of canopy).

The TanDEM-X and SRTM missions were conceived to acquire interferometric datasets that would allow the generation of surface elevation models (Farr et al., 2007; Krieger et al., 2007). Over forested terrain, an estimate of vegetation height can be inferred from the surface elevation if the terrain elevation is known. To obtain the true vegetation height, an additional step that compensates the InSAR-based height of the vegetation for the penetration of microwaves into the canopy is required (Walker et al., 2007). Although high resolution, accurate surface elevation models based on interferometric data exist, there is no global dataset of terrain elevation, which hinders the use of interferometry for a “direct” measure of the vegetation vertical structure. It will not be until the BIOMASS mission is flying that estimates of ground elevation may be possible (Quegan et al., 2019), although the coverage will not be global (Carreiras et al., 2017) and will be at a coarser spatial resolution than the CCI Biomass products (Quegan et al., 2019). To the best of our knowledge, there is no spaceborne mission planned that can provide a global estimate of terrain elevation.

Laser instruments also measure the elevation of the Earth surface and, in the case of vegetation, return a profile of reflection intensity along the vertical direction. The GLAS instrument on-board the ICESat satellite operated between 2003 and 2009 and recorded millions of waveforms along its orbital path. Unlike interferometric datasets, the signal recorded by a laser instrument contains also a ground return, so that an external dataset of terrain elevation is not required to estimate the height of vegetation. Waveform information in the GLA14 product was processed globally in the GlobBiomass project [RD-8] from which canopy density and several height percentiles were computed. A GLAS footprint has an approximately 70 m diameter and footprints were acquired sequentially along an orbit; however, the distance between orbits was around 60 km, leading to a sparse sampling of the Earth’s vegetation. For this reason, it is preferred to use the GLAS datasets of canopy height and canopy density to derive models in support of the retrieval model relating SAR backscatter and AGB rather than as surrogate reference data for model training.

Since 2018, the GEDI and ICESat-2 laser systems have been providing observations with a much denser coverage of the Earth land masses than ICESat GLAS. We have therefore tested the contribution of data from these recent missions to the models. In spite of the much denser coverage, our retrieval approach does not foresee estimation of AGB based solely on the LiDAR observations as this is already taken care of, for example by the GEDI team. Our understanding is also that retrieval of AGB should combine multiple observations from spaceborne SAR, optical and laser observations and exploit the information content on AGB in each set of observations.

The data providers warn about the use of some of their measurements (Neuenschwander and Pitts, 2019; Dubayah et al., 2020) in early data versions. With the advance of processing routines by the data providers, the accuracy of the laser measurements will improve. Another reason for following closely the development of data products by the GEDI and ICESat-2 teams is their interest in releasing global datasets of forest variables, including AGB. Recent estimates of AGB based on GEDI are available either at footprint level or as aggregated values in 1 x 1 km^2 large grid cells. The Biomass Harmonization activity is currently assessing CCI Biomass and GEDI AGB products to create knowledge and allow for improvements of the individual data products.

4.2. Characterizing the AGB - LiDAR height model

In the CORE algorithm developed since Year 2, we have introduced models linking AGB with top-of-canopy height in the WCM. The characterisation of this power-law function was based on the ICESat GLAS top-of-canopy height measurements (RH100) and the GlobBiomass AGB dataset. Although the trend between AGB and RH100 was, on average, similar to results based on measurements at local scale, there is substantial work needed to: (i) reduce uncertainties and (ii) improve the spatial characterisation of the model parameters. Studies at local sites allow determination of precise models, but these may not be generalisable to larger areas. Remote sensing maps, in contrast, allow us to obtain a region-wide perspective on how height and AGB are related but these relationships may be locally inaccurate. The availability of dense sets of LiDAR observations of RH100 (and in general, different height metrics) from GEDI and ICESat-2 allowed a more detailed characterisation of AGB-to-height model, which however suffered from the early versioning of the data, implying that some height ranges may exhibit deficiencies. While the accuracy of the ICESat-2 and GEDI datasets will improve, there is a need to understand how well we can characterise the model spatially. Here, we identify local models, such as those developed in the context of CCI Biomass from airborne laser datasets and plot inventory data [RD-5], as a diagnostic tool for the map-based model. However, in regions poorly covered by LiDAR observations, it will still be impossible to quantify the reliability of the map-based model.

4.3. Characterization of tree attenuation

Having fixed the functional dependencies between height and AGB on one hand, and canopy density and height on the other, the WCM becomes invertible once the coefficients, σ^0_{gr} and σ^0_{veg}, and the two-way tree attenuation coefficient, α, have been estimated. A new approach for estimating the unknown WCM parameters is tested in which the three unknown parameters are estimated by fitting Equation 4-1 (see also [RD-5], Equation (4-1)) to observed relationships between backscatter and canopy density:

$$\sigma^0_{for} = (1-\eta)\sigma^0_{gr} + \eta\sigma^0_{gr}e^{-\alpha h(\eta)} + \eta\sigma^0_{veg}\left(1 - e^{-\alpha h(\eta)}\right) \tag{4-1}$$

where η is the area-fill or canopy density factor and the height term is expressed as a function of η (see [RD-5], Equation (3-6)) by:

$$h = -\frac{\log(1-\eta)}{q} \tag{4-2}$$

Possible dependence of the parameters on the local incidence angle is dealt with by fitting separate models for different incidence angle intervals Figure 4-1. Figure 4-2 illustrates the range of values for the two-way tree attenuation coefficient α obtained by fitting Equation 4-1 to observed relationships between ALOS-2 L-HV backscatter (year 2018 mosaic) and Landsat canopy density. The spatial distribution of the derived estimates reveals distinct regional differences. Low values for α, mostly less than 0.5 dB/m, are obtained primarily in boreal forest regions. In temperate and sub-tropical forests, the estimated values for α tend to exceed 1 dB/m. While the range of values obtained seems reasonable, in particular in the boreal zone, it remains unclear if the observed regional differences reflect actual differences in attenuation or rather properties/errors of the Landsat canopy density product. A sensitivity analysis was carried out to evaluate the effect of the attenuation coefficient on the multi-temporal AGB retrieval in different forest regions. A comparison of L-band radar-derived AGB estimates against LiDAR maps of AGB suggested that a fixed value of 0.5 dB/m for the attenuation coefficient, which has so far been assumed universally in the CORE algorithm, represents a reasonable choice for most forest types. However, in the wet tropics and sub-tropics a fixed value of 0.5 dB/m is associated with underestimation of high AGB ranges and therefore in the Year 3 implementation of the CORE algorithm we opted to use instead a fixed value of 1 dB/m in the latitude ranges between 23° S and 23° N. A direct use of the estimates for α obtained by fitting the model in Equation 4.1 to observations of L-band backscatter as a function of Landsat canopy density did not improve the AGB mapping despite spatially adapting to potential regional differences in attenuation. Further improvements of the CORE algorithm by better characterisation of differences in forest attenuation in the retrieval therefore requires further investigation based, for instance, on a dense set of estimates of canopy density and height derived from GEDI or ICESAT-2.

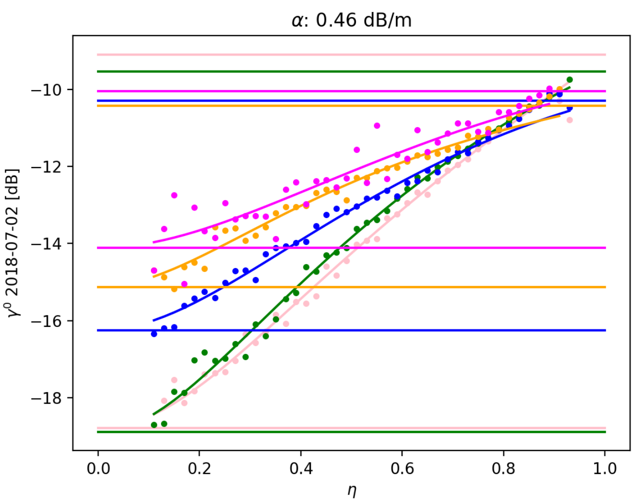

Figure 4-1: Observed and modelled relationship of L-HV backscatter as a function of Landsat canopy density. The model in Eq. 4-1 was fitted with variable transmissivity for different incidence angle ranges (pink: 20-30°, green: 30-40°, blue: 40-50°, orange: 50-60°, purple: 60-70°). For each incidence angle range, the horizontal lines denote the level of the estimated γ^0_{gr} and γ^0_{veg}.

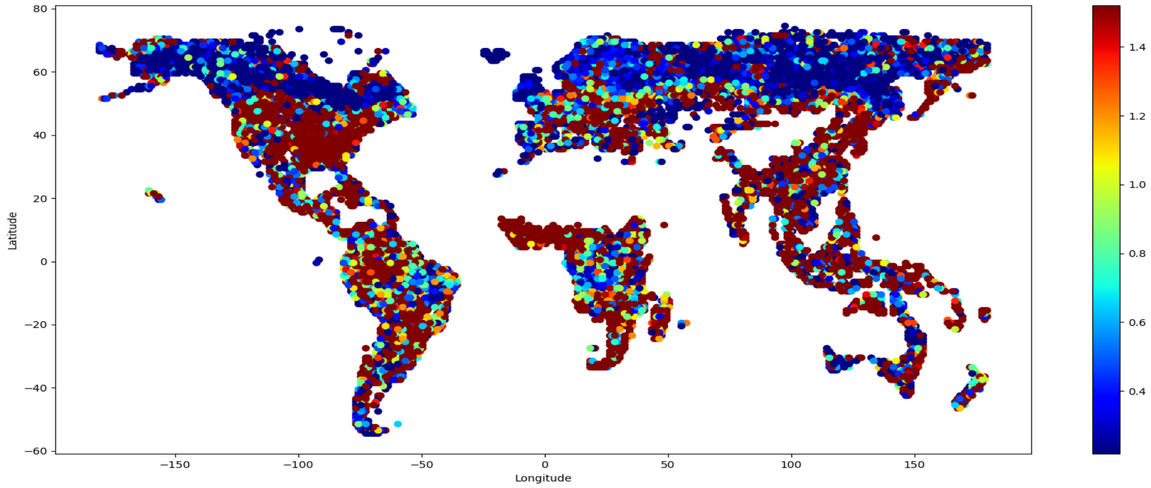

Figure 4-2: Estimates of the two-way forest attenuation coefficient α [dB/m] obtained by fitting Equation 4-1 to observed relationships between L-HV backscatter and Landsat canopy density.

4.4. Use of vegetation structural information

One of the limitations of the currently implemented BIOMASAR algorithms is the coarse representation of vegetation structure. In Year 1, some of the model parameters were estimated after stratifying the world by the Food and Agriculture Organisation (FAO) ecological zones. In Year 2, we introduced a finer stratification based on subdivisions of 883 ecoregions to characterise the relationship between canopy density and RH100 but still used ecological domains to characterise the relationship between RH100 and AGB. Vegetation structural information developed in the DARD [RD-3] should provide more targeted estimation of model parameters and models.

In the same vein, knowledge gathered by investigating the relationship between EO observables and AGB in specific forest classes should be exploited. When evaluating the GlobBiomass and the CCI Biomass map (Year 1) in mangrove forests, the specific scattering mechanisms occurring at C- and L-band were not correctly accounted for in the retrieval model. The AGB of mangroves was often underestimated because the absorption of microwaves in the canopy leads to low backscatter. The same reasoning applies to plantation forests. The reliability of the AGB map products is unknown because the validation activities have not covered such vegetation types due to the lack of suitable data available to the validation team.

4.5. Use of coarse resolution EO data

From the analyses reported in previous validation reports, estimation of AGB of high AGB forests still needs to be improved. Observations from coarse resolution sensors operating at C- and L-band, such as Advanced Scatterometer (ASCAT), Soil Moisture and Ocean Salinity (SMOS) and Soil Moisture Active Passive (SMAP), have tremendous potential to improve AGB estimates. However, these datasets have a spatial resolution that ranges between 25 km and 50 km. It is unclear whether estimates at such coarse resolution can be transferred to 1 ha. In this respect, the experiences by the soil moisture community concerning the re-scaling of coarse resolution soil moisture fields to high resolution maps could inform a similar strategy when estimating AGB.

5. Advancing the estimation of AGB changes

5.1. Introduction

In v3 of the Algorithm Theoretical Basis Document (ATBD) of CCI Biomass, the approach adopted for assessing AGB change between two epochs was based on differencing AGB estimates between years (the stock-difference method), with consideration given to their uncertainty. This approach was adopted as global AGB products had only been generated for 2010 and 2017/2018. However, in v4, the maps of AGB for these years were updated and new layers were generated for 2019 and 2020, with these allowing investigation into the trends in AGB. Hence, new methods for ascertaining the directions and magnitudes of AGB changes and associated uncertainties could be explored over the period 2010 / 2017-2020. Those currently selected are presented herein.

Changes in AGB can manifest themselves in diverse ways across the world through an often-complex combination of factors, including the timing of the change, the nature and intensity of the causal agents, the response of forests to the change, and interactions with the surrounding environment. Earth Observation data collected with space-based instruments are not always consistent and can be subject to errors that lead to uncertainties in classifications of landscapes or modelled estimates of biophysical variables. These limit our ability to ascertain the extent to which the change detected corresponds to what has happened on the ground. As the ESA CCI AGB estimates are affected by these uncertainties, which can be substantial, we propose to bring the currently selected methods (stock-difference and trend analysis) within an existing evidence-based approach developed through the *Living Earth* project (Lucas *et al*., 2022). This framework describes change on the basis of impacts and driving pressures inferred from diverse Earth Observation data. The ESA CCI AGB estimates can be used in conjunction to support whether changes, detected through time series comparisons, agree with, and can be explained through the evidence accumulated from these Earth Observation data (e.g., relating to climate, land management or biogeography).

5.2. Methods

The two approaches currently identified and adopted for detecting and describing changes in AGB between epochs are the stock-difference method, which involves simple differencing with the standard deviation as a measure of uncertainty, and the Mann-Kendall (Kendall, 1938, Mann, 1945) Theil-Sen slope (Theil, 1950; Sen, 1968) methods, which allow the detection of monotonic trends and their slope. These methods are described in more detail in the following sections.

5.2.1. Stock difference method

As demonstrated for v3, a straightforward way of estimating AGB change between two epochs is to calculate the difference between two AGB maps, which can be time-separated by a year (e.g., 2017 and 2018) or a decade (e.g., 2010 and 2020). The significance of the change can be accounted for by using the standard deviation around the estimated AGB means for the two dates or epochs being compared. If these error bars do not overlap (Figure 5-1), the AGB difference can be considered statistically significant under the assumption of unbiased estimates or equal biases in both AGB stock maps. If they overlap partially or fully, a potential or improbable change is indicated.

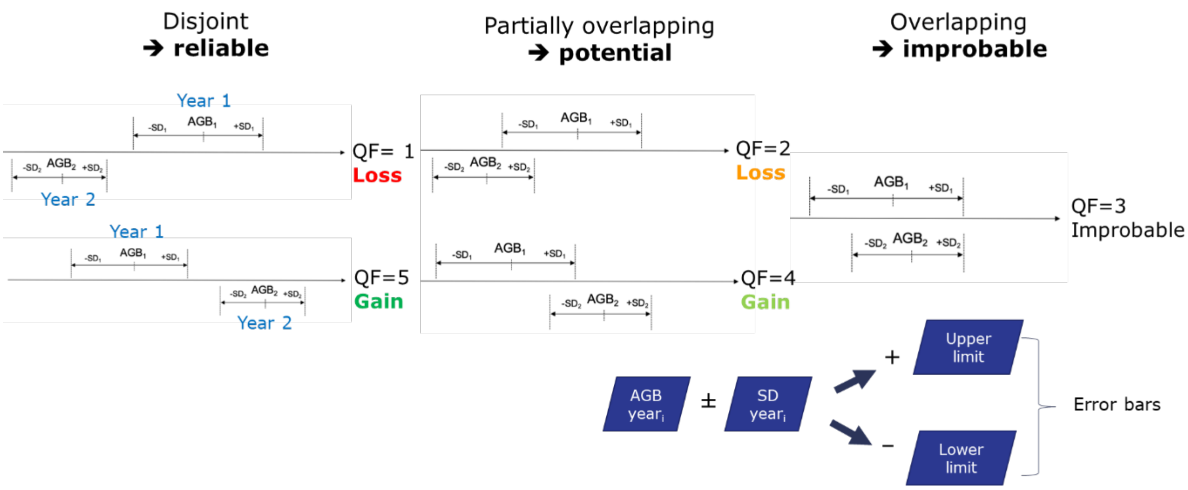

Figure 5-1: Overview of the stock-difference approach to AGB change detection.

The standard deviation, reflecting the precision of the stock-difference estimate, is calculated as the square root of the sum of the variances of the two individual maps, which assumes the errors in the two estimates are independent. This standard deviation can then be used to generate a quality flag for the difference estimates (i.e., reliable, potential or improbable change), which assists with the interpretation of the significance of the difference detected for an area. Both the standard deviations of the change and the quality flags are currently provided by the ESA CCI BIOMASS CRDP alongside the AGB and standard deviation for each year.

There are a number of drawbacks to the stock-difference approach, which include:

a) The change that can be detected depends on the standard deviations of the individual AGB estimates. The larger their values, the wider the spread about the mean and thus the more likely the standard deviation intervals will overlap.
b) Biases in the individual AGB estimates will propagate to the AGB difference estimate, and the variance of the estimated difference will be larger than that of each individual estimate. Both bias and precision issues were identified and discussed in the ATBD and PVIR, and both affect the quality of the AGB difference estimated from the CCI BIOMASS AGB data products.
c) CCI BIOMASS generates maps of AGB by combining data from different sensors, namely ENVISAT ASAR and ALOS PALSAR for 2010 and the Sentinel-1 and ALOS-2 PALSAR-2 for 2015 onwards, and this introduces errors that may be difficult to identify and quantify.
d) Depending on the frequency, polarisation and other factors (e.g., incidence angle, moisture content of vegetation and soils), the radar signal saturates and sensitivity to differences in AGB decreases near the saturation level. Similarly, the capacity to detect changes in AGB between dates or epochs may be compromised as measurements may also be affected by environmental conditions at the time of observations.
e) Only net changes in AGB over large temporal intervals between observations (e.g. decadal) are detected, with fluctuations at finer temporal intervals often not identified.

In CCI BIOMASS, global, repeated observations from multiple spaceborne missions are found to have substantially higher predictive power and hence, as more AGB estimates become available, the opportunities for trend analyses are increased.

5.2.2. Trend analysis

Where more than two estimates are available, trends in AGB can be used to identify whether there is an increase, decrease or no change between the periods of retrieval, noting that over long time series, these trends may not be monotonic. Methods for establishing whether trends over time series observations are significant include repeated applications of the stock difference method (as described above) or the non-parametric Mann-Kendall test and Theil-Sen slope.

a) Multiple comparisons of stock-difference estimates:

Between successive years (e.g., 2017 to 2018, 2018 to 2019 and 2019 and 2020), the significance of the difference in AGB is assessed and collated for each year to establish whether there is no change or there are successive gains or losses or combinations of these (Figure 5-2). These are summarised for the final year of interest (here 2020) to highlight whether there has been a net gain or loss in AGB overall based on the significance of difference, with interruptions to the sequence identified. This could also result in the generation of successive quality flag assessments and standard deviations of differences between years. The large time-interval between 2010 and 2017 onwards may compromise this approach because of natural events/processes or human activities that might have occurred from which forests may (or otherwise) have recovered sufficient AGB for these not to be detected.

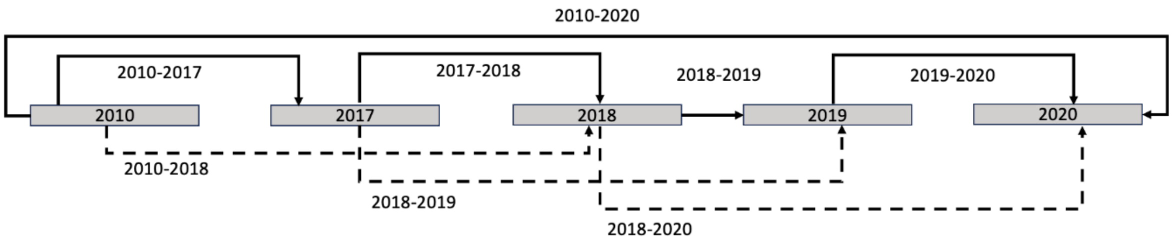

Figure 5-2: Repeated comparisons of stock-difference estimates and associated uncertainty metrics over time series of AGB maps can be used to determine relative magnitudes and directions of change.

b) Mann-Kendall and Theil-Sen slope:

The non-parametric, non-seasonal Mann-Kendall test can be used to detect if there is a decreasing or increasing monotonic trend in multi-temporal AGB estimates and evaluate the significance of this trend (Kendall, 1938; Mann, 1945). This method calculates the sign of the change between each pair of AGB estimates compared, giving 1 or -1 for a gain or loss respectively, or 0 if both values are equal, (Equation (5-1), Gilbert, 1987). The signs of all pairs are then summed for all the year intervals, with this indicating whether AGB is increasing or decreasing overall. This can be calculated as follows:

$$S = \sum_{k=1}^{n-1} \sum_{j=k+1}^{n} sign\,(x_j - x_k) \tag{5-1}$$

$$sign\ (x_j - x_k) = \begin{cases} +1 \text{ if } x_j - x_k > 0 \text{ (gain)} \\ 0 \text{ if } x_j - x_k = 0 \text{ (no change)} \\ -1 \text{ if } x_j - x_k < 0 \text{ (loss)} \end{cases}$$

Here, n is the length of the time series and x_j and x_k are the measurements observed at years t_j and t_k.

The Theil-Sen slope estimator (Theil, 1950; Sen, 1968) determines both the direction (increasing or decreasing) and magnitude of the change and is calculated as the median of all possible slopes among data pairs in the time series.

$$MEDIAN\left(\sum_{k=1}^{n-1} \sum_{j=k+1}^{n} \frac{(x_j - x_k)}{(t_j - t_k)}\right) \tag{5-2}$$

where x_j and x_k are the measurements at years t_j and t_k.

The variance of the Mann-Kendall statistic can be estimated as follows:

$$\mathrm{VAR}(S) = \frac{1}{18}\left(n(n-1)(2n+5) - \sum_{k=1}^{g}(F_k(F_k-1)(2F_k+5)\right) \tag{5-3}$$

where g represents the number of tie groups (i.e., repeated values observed) and F_k the number of times these values appear in the k-th tie group.

The significance of the trends over the selected time series can be determined using the standard normal statistic, z, which is calculated by dividing the Mann-Kendall statistic by its standard deviation (based on a two-sided test).

$$z = \begin{cases} \frac{S-1}{\sqrt{VAR\ (S)}} & \text{(S>0) increasing trend} \\ 0 & \text{(S=0) no change} \\ \frac{S+1}{\sqrt{VAR\ (S)}} & \text{(S<0) decreasing trend} \end{cases} \tag{5-4}$$

The probability of observing an extreme value (i.e., the P-value of z) of the Mann-Kendall statistic is calculated as (Clinton, 2020):

$$Pvalue = 1 - P(|z| < Z) \tag{5-5}$$

For a two-sided test to establish whether a positive or negative trend exists at the 95% confidence level, the P-value is compared to the value of 0.975. Pixels indicating a significant trend can be highlighted by using a mask where the P-value is within a specified threshold (e.g., P-value lower than 0.025, 0.05, or 0.001) and hiding the pixels outside this threshold (Clinton, 2020).

The CCI Biomass AGB estimates are generated from time series of C- and L-band SAR data and are aggregated on an annual basis. They are thus assumed minimally affected by seasonality, which is a requirement for using the non-seasonal Mann Kendall test. We also assume that the AGB estimations are not serially correlated over time. The combination of the Mann-Kendall and Theil-Sen slope is robust to outliers but a minimum of three time-separated estimates of AGB are required. Other drawbacks to using the Mann-Kendall and the Theil-Sen slope include:

a) The approach is not applicable where the intervals between observations are not consistent over time (e.g., AGB data missing for years 2011-2016)
b) It is sensitive to ties (repeated identical values) which may lead to small Sen's slopes being rounded to 0 even if the trend is flagged as significant by Mann Kendall test.
c) It is sensitive to autocorrelation and seasonality in the time series.
d) It may miss true trends for shorter time series with an insufficient frequency of observations

As with the stock-difference approach, an increase in AGB at decadal points only might indicate no change in AGB but forests may have been cleared or degraded then recovered subsequently during the intervening period so that no change is detected. The assumption of no change is likely to be most frequently observed for forests that are of low AGB (e.g., shrublands) or that rapidly accumulate AGB (as in the case of tropical regenerating forests) even though a substantive loss might have occurred during a change event. Similarly, where the radar backscatter is above a saturation level, any growth in the intervening period is unlikely to be captured.

5.3. Integrating stock-difference and/or trend analyses in evidence-based change frameworks.

Differences in AGB retrieved between two dates or epochs, or in observed trends contribute evidence of complete or partial losses or gains of forest carbon (or no change), with the estimates of dispersion giving confidence, or otherwise, of impacts on carbon budgets and cycles over varying time periods. Time becomes an important contributor to the evidence base, as changes may be fast (ranging from hours to weeks) or slow (weeks to decades). Time series comparison of maps and descriptions of land cover also provides evidence as to whether a forest has experienced conversion (i.e., a change in broad land cover extent) or modification (a change in vegetation type or amount) with both likely to affect changes in AGB.

Complete losses of AGB are associated with the conversion of forests to a new land cover (e.g., cultivated, bare or urban), with deforestation, urban expansion and severe bushfires being common causes that often occur over a relatively short time period. It is important to be mindful of the difference between land cover and land use. For example, complete losses of AGB occur during clearcutting on 'forest land remaining forest land', where the land use remains the same, but the land cover changes during the timber harvesting. Uncertainty in the amount of AGB lost is related directly to the error in the retrieval of AGB prior to what is a natural event or human activity. By contrast, partial losses in AGB result from modifications of the forest (e.g., through selective logging, thinning or natural dieback). In this case, uncertainties in detection are based on those determined using the methods applied to generate comparisons, including stock-difference or trend analyses. These partial losses are often rapid but may also occur over longer time periods, particularly in the case of forest degradation (e.g., through fuelwood gathering, insect infestations or disease).

Gains of AGB are only rapid if there is direct planting of trees, but the remotely sensed signal from these generally only becomes evident after several years when at optical wavelengths or C-band but may require at least 5-10 years of growth to be visible at L-band. Growth rates vary, however, with climatic, edaphic, topographic and geological settings, the biogeographical distributions of species and possible human use and management of the land either prior to or following forest establishment. Direct planting of larger or a high density of trees will evoke a signal once completed but is uncommon.

Whilst not affecting quantification of the losses and gains in AGB and not directly used to assess uncertainty, evidence gathered from a range of sources can be used to confirm or better establish whether the magnitude and directions of AGB change agree with that observed in other biophysical attributes (e.g., canopy cover or height) or surrogates of these (e.g., vegetation indices or fractional covers). Furthermore, knowledge of the causes of change, whether from natural events or processes and/or human activities in different geographical areas, can assist in the understanding and interpretation of change. The uncertainty in the estimation of all contributory elements to the evidence base can also be used to give greater confidence in any assessments of AGB change. The framework developed through *Living Earth* provides an opportunity to undertake this assessment.

5.3.1. A proposed framework for evidence-based change.

Living Earth has been developed as a concept and framework for mapping and describing land covers and detecting change based on evidence, primarily from Earth observation data. This established but evolving approach has been applied to Australia (Owers *et al*., 2020), Papua New Guinea and Wales, and the United Kingdom (Planque *et al*., 2020).

Living Earth constructs and further describes land cover classes from environmental descriptors retrieved or classified from Earth observation data processed into Analysis Ready Data (ARD) and according to the FAO Land Cover Classification System (LCCS Version 2.0; di Gregorio (2005)). A strict condition is that contributing environmental descriptors have defined units (e.g. m, %, Mg ha^{-1}, time) or categories (e.g. species codes), which gives independence of space (scale) and time. Environmental descriptors are differentiated into those that are overarching, essential or additional.

- Overarching environmental descriptors (OEDs) are used to define (and map) the broad land covers (agriculture, semi-natural vegetation and artificial and natural bare surfaces and water) of the FAO LCCS and include the fractional cover of photosynthetic or non-photosynthetic vegetation (%) and water hydroperiod (time) or classified urban extent (e.g. from radar).
- Essential descriptors are required to generate, in part or fully, the FAO LCCS classes (approximately 12,000 in total, with each having biophysical meaning). These include lifeform (woody, herbaceous), leaf type (broadleaf/evergreen), vegetation phenology (deciduous, evergreen), and annual water hydroperiod.
- Additional descriptors further describe the land cover, with examples being crop type (Planque *et al*., 2021), dominant tree species or forest community, and contextual information such as peat depth, geology and soil acidity (Punalekar *et al*., 2023).

AGB is regarded as an Additional Environmental Descriptor but can be ingested as it has the continuous unit of Mg ha^{-1}. Hence, the AGB maps generated by CCI BIOMASS can be used to describe forested area mapped as such for 2010 and for each year from 2017 to 2020 and beyond. An example of their integration is given in Figure 5-3, which shows land cover for a section in Wales (United Kingdom) and the associated estimate of AGB.

A)

B)

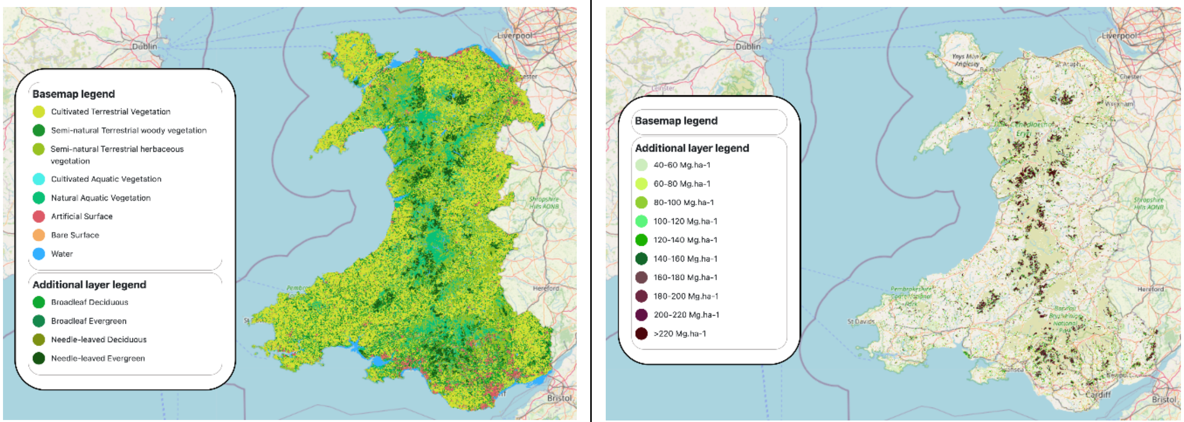

Figure 5-3: a) Land cover map of Wales (UK) generated at 10 m spatial resolution from Sentinel-1 and Sentinel-2 data, highlighting the FAO LCCS Level 3 (Overarching Environmental Descriptors) and the forest leaf type/phenology and b) the CCI Biomass AGB maps at 100 m. Both maps were generated for 2020.

To describe change, *Living Earth* partners (informed by CCI BIOMASS) developed a globally applicable Evidence Based Change Framework and Global Change Taxonomy, which was designed for global application and builds on the Driver-Pressure-State-Impacts-Response (DPSIR) framework (Oesterwind *et al.*, 2016). The taxonomy (Figure 5-4) lists 77 impact and 144 pressure classes that, when combined, give 248 'impact (pressure)' classes, each of which can be evidenced by accumulating and comparing changes in states (i.e., the Environmental Descriptors used to construct and further attribute the land cover categories). Examples highlighted in Figure 5-5 include vegetation dieback (the impact) as a consequence of strong winds, pathogens, sea level fluctuation or low intensity bushfires. The Evidence-Based Change Framework provides a basis for collating the evidence for both change impacts and pressures, with these obtained spatially and over time from Earth observation data but also a range of other spatial and, in some cases, non-spatial datasets. Time is included as a contributory descriptor relevant for differentiating short-term natural events or human activities (e.g., vegetation amount loss as a consequence of bushfires or deforestation) or longer-term natural process (e.g., vegetation gain through growth). Furthermore, the contributory evidence can be supported by estimates in the uncertainty of retrieval or classification of continuous or categorical environmental descriptors respectively.

5.3.2. Regional demonstration (Wales and Australia).

In Australia, time series of 30 m spatial resolution Landsat sensor data (Collection 3), processed to an ARD format have been accumulated within Geoscience Australia's Digital Earth Australia (DEA) and the Open Data Cube (opendatacube.org). From these, environmental descriptors have been classified or retrieved for each year and used to construct summary classifications of land cover (for the Australian continent and islands) annually from 1988 to 2022. These maps are available through DEA (https://maps.dea.ga.gov.au/story/DEALandCover) and can be analysed within DEA's Sandbox (https://app.sandbox.dea.ga.gov.au/). For Wales, the same software and approach has been developed within the new Welsh Data Cube (WDC) to generate land cover maps with the same legend, annually from 2018 to 2022 (https://earthtrack.aber.ac.uk/livingwales/maps.html).

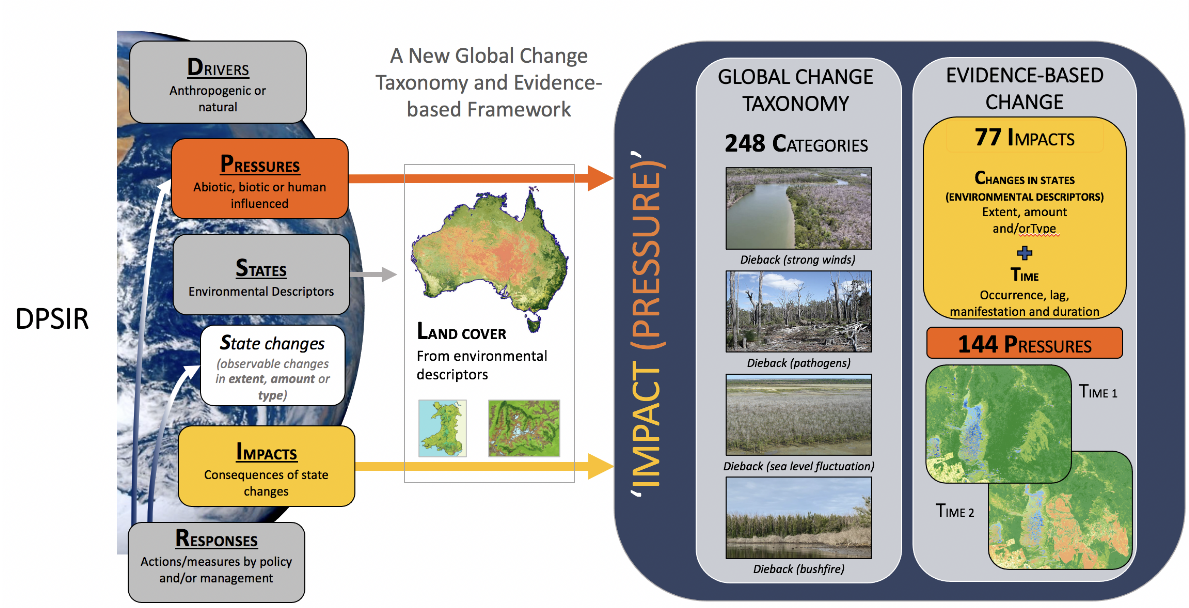

Figure 5-4: The Global Change Taxonomy and Evidence Based Change Framework (Lucas *et al.*, 2022) that builds on the Driver-Pressure-State-Impacts-Response (DPSIR) framework.

ESA CCI Biomass AGB maps for 2010 and annually from 2017 to 2020 have been ingested into the user workspace of DEA (with the latter also integrated within the WDC) and compared alongside the land cover maps and environmental descriptors for each year, with the latter providing supportive evidence for changes in forest AGB. These changes in broad land cover classes in terms of both extent (off-diagonal) and amount or type (on-diagonal) can be represented and distinguished by a transition matrix (Figure 5-6).

Type includes the lifeform classes of woody (trees and shrubs) and herbaceous (grasses, forbs, lichens and mosses) and of note is that inclusion of these allows translation to the Intergovernmental Panel on Climate Change (IPCC) Agriculture, Forestry and Other Land Use (AFOLU) categories. Furthermore, the eight OEDs in addition to the two lifeform classes of woody and herbaceous can be mapped from Earth observation data.

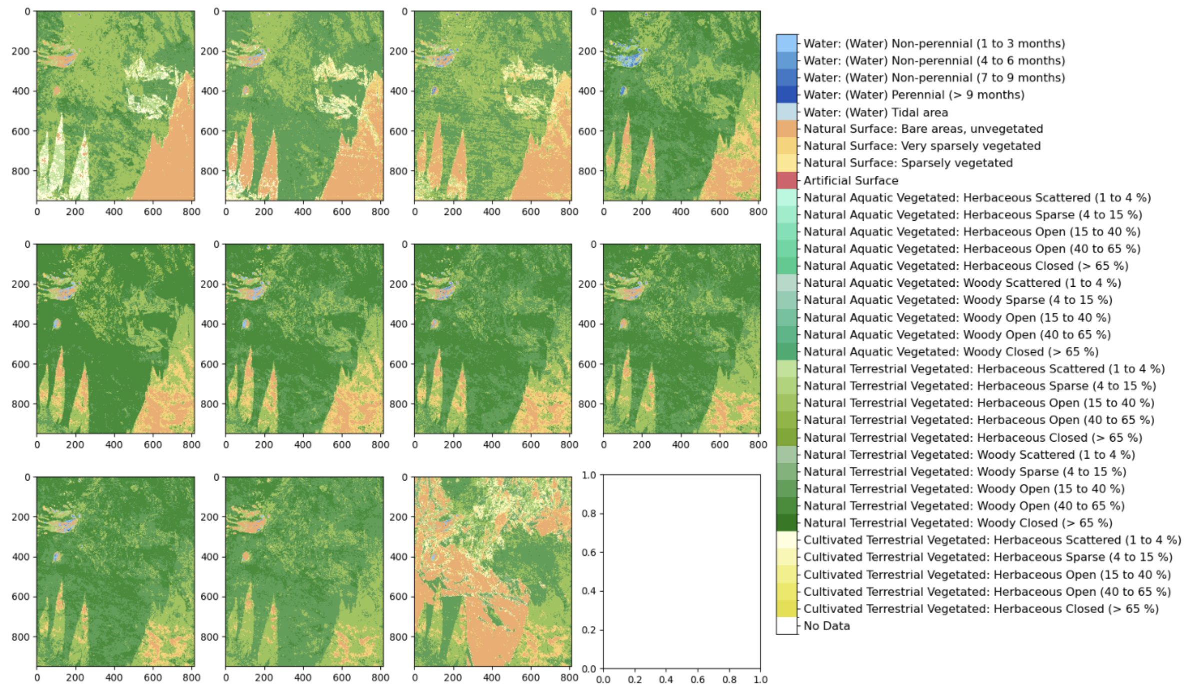

Figure 5-5: Land cover maps generated for Mt Ney, Western Australia, for 2010 to 2020 (top left to bottom right), with these generated from environmental descriptors retrieved or classified from Landsat sensor data and according to the FAO LCCS.

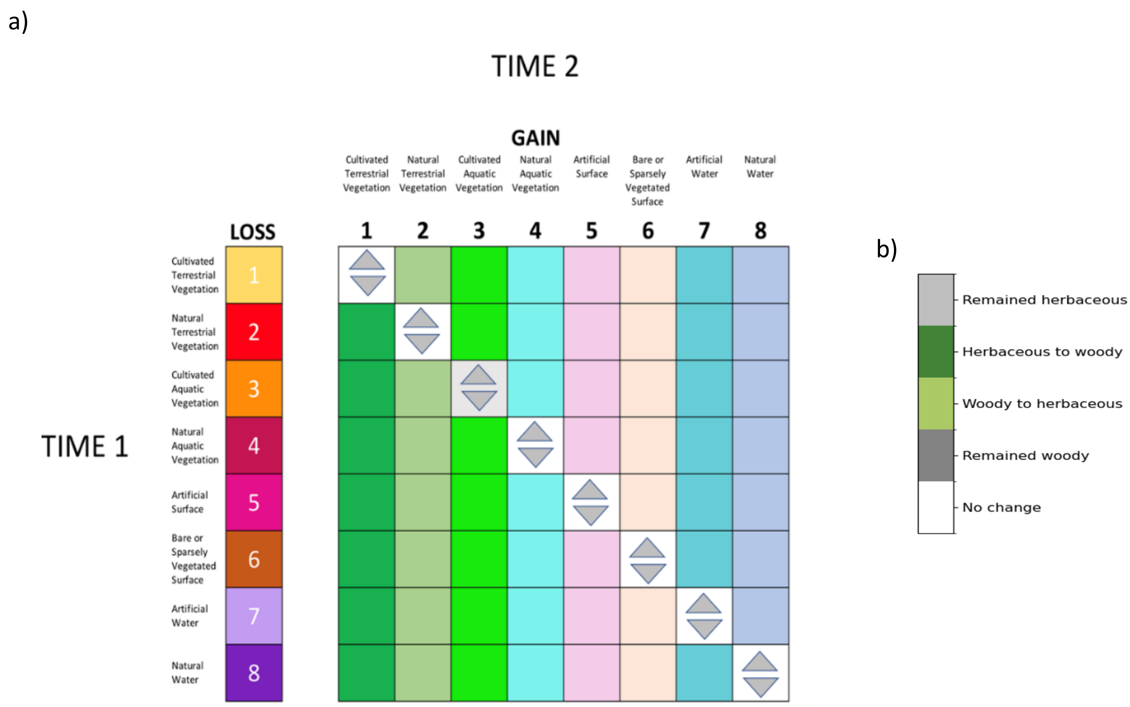

Figure 5-6: a) The transition matrix between FAO LCCS Level 3 classes indicating both off-diagonal (extent) and on-diagonal (type or amount) changes and b) changes in overarching lifeform types (woody and herbaceous).

Comparisons of the OEDs (broad land covers) through the transition matrix allow differentiation of:

a) Areas associated with a gain (Figure 5-7a) or loss (Figure 5-7b) in the extent of land covers over the period of comparison, with these typically linked to complete removal of AGB or an increase in AGB on areas previously not supporting forest. However, the detection of changes in AGB depends on whether there is sufficient time for the same or a new land cover to recover AGB (if at all) including to pre-loss levels.
b) Areas where the land cover has remained the same (Figure 5-7c; e.g., natural to semi-natural terrestrial or aquatic vegetation) but a change in type (Figure 5-7d; e.g., from woody to herbaceous lifeforms or *vice versa*) or amount (including AGB; e.g., Figure 5-7e) has occurred.

In both cases, evidence can be accumulated by comparing the land cover maps and the environmental descriptors used in their construction and description (including in terms of AGB) over time. Uncertainties in the estimates of these descriptors and their changes can be included to give confidence in the nature, magnitude and direction of change, including those based on stock-difference and trend analyses (Mann-Kendall and Theil-Sen slope).

The *Living Earth* system allocates unique codes to each of the categorical OEDs, EDs and AEDs but also considers values for continuous variables, such as those associated with AGB (Mg ha^{-1}), canopy cover (%) and vegetation height (m). These codes are gathered to build evidence for the change (i.e., impact). Whilst there are 77 impact categories listed in the Global Change Taxonomy, only 32 relate to forests.

The unique codes for each ED, which can be represented as numbers in a single raster layer, are based on the FAO LCCS coding system (e.g., 1 for woody (B1) and 2 for herbaceous (B2) lifeforms). Changes in one or more of these descriptors can occur over different time-separated periods (e.g., sub-annually, annually or decadal), with these indicated by a change in the numeric value in one or more of the corresponding layers. Where all characteristics of a forest remain the same, the codes are unchanged between the first and second epochs, but if one or more descriptors change (e.g., the canopy cover reduces from > 60% (A12) to < 15% (A16)) for the second period, then the values will be different (i.e., changing from 12 to 16 in the case of the canopy cover layer). The continuous values of canopy cover (%; if available) can also be compared to give greater fidelity in the description of change. In generating evidence for an impact, individual ED layers of relevance, as suggested in the evidence base of the change framework (https://github.com/livingearth-system/Globalchangeframework), are compared between the different epochs, and the difference (if any) is represented as the concatenation of the codes from each time slot compared. The uncertainty in the classification of categorical or retrieval of continuous EDs can also be included in this evidence base, with these individually or in combination, giving confidence in the assessment of change. This assessment allows the impacts of change to be differentiated, described and quantified numerically.

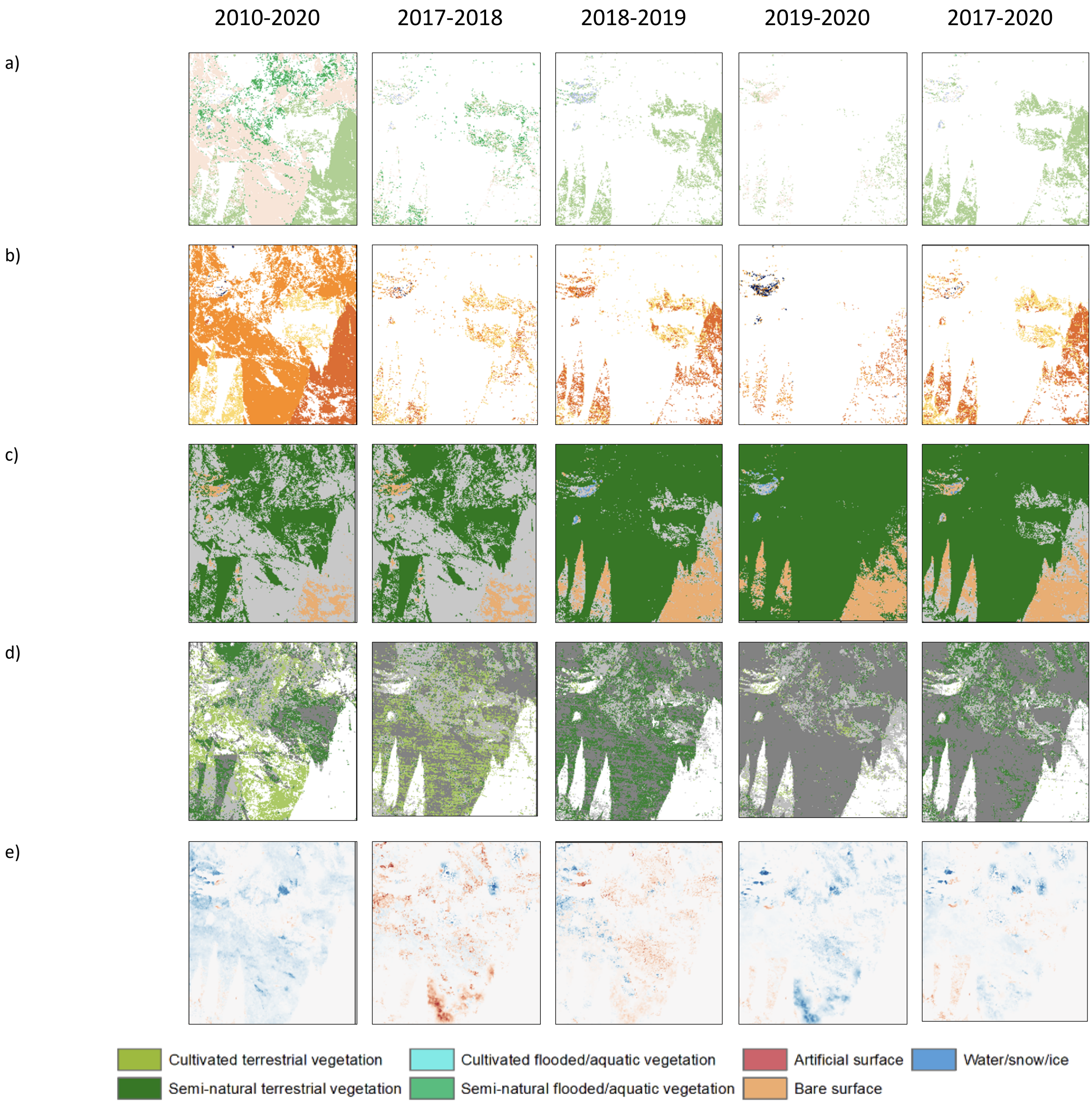

Figure 5-7: a) Gains and b) losses and c) no changes in broad land cover classes (OEDS = Overarching Environmental Descriptors); changes in d) lifeform (woody and herbaceous) categories and e) AGB (losses=blue, gains=red). Legends for a, b and d are in Figure 5-6. The full standardized legend for c) is provided in this figure, noting that bare surface and semi-natural vegetation are dominating.

The changes observed In the OEDs that are represented in the transition matrix in Figure 5-6 can indicate a change (loss or gain) or otherwise in the extent of the Level 3 classes of the FAO LCCS. The extent changes can again be represented by concatenated numbers from the two times being compared. For example, cultivated terrestrial vegetation (CTV) and natural/semi-natural terrestrial vegetation (NTV) are assigned codes of 111 and 112 respectively (collated from individual codes representing vegetated (1), terrestrial (1) and cultivated (1) and natural/semi-natural (2) respectively at Levels 1, 2 and 3). Hence, transitions from CTV to NTV can be represented as the integer value 111112 whereas when there is no change, then the combined code is 111111 or 112112 respectively. However, in the latter case, an increase or decrease in amounts (e.g., AGB) or types of materials (e.g., lifeform, leaf type and/or phenology) may occur. For example, a change in lifeform from woody to herbaceous or *vice versa* can be represented by the codes 12 and 21 respectively and 11 and 22 if there is no change between the periods being compared. Similarly, estimates of other descriptors (including AGB, canopy cover) over time and the significance of change based on their uncertainties) can be included. Hence, there is capacity to build up sequences of numbers which can be used to collectively indicate the impact, of which there are 32 (as indicated above).

An example of this concept is given in Figure 5-8, which highlights how the values for contributory environmental descriptors have been collated to provide evidence of four change impacts near Mt Ney in Western Australia, namely vegetation amount (loss), vegetation extent (loss), vegetation amount (gain) and vegetation extent (gain). These are then combined to provide what is termed an 'impact' layer, which (in this example) has 4 values (44, 45, 46, and 47) but can be up to 32 or 77 respectively if just forests or all environments (e.g., agriculture, water, bare, artificial and non-woody herbaceous) are considered.

Of the 144 pressures listed in the Global Change Taxonomy, 46 lead to one or more of the 77 impacts on forest extent or states. To associate these with impacts, these are similarly numbered (i.e., 1 to 144) and then concatenated onto the impact number to create a five-digit number that provides a consistent description of the 248 'impact (pressure)' categories. These can be established from a range of sources (Lucas *et al*., 2022), including those generated by other ESA CCI products (e.g., land surface temperature, fire, snow cover, sea level). The impact and driving pressures can also take place simultaneously or sequentially. For example, vegetation dieback may be the consequence of both drought and pathogens whilst vegetation damage through strong winds might be followed by vegetation damage because of flooding. The timings and durations of a range of 'impact (pressure)' categories can therefore be considered.

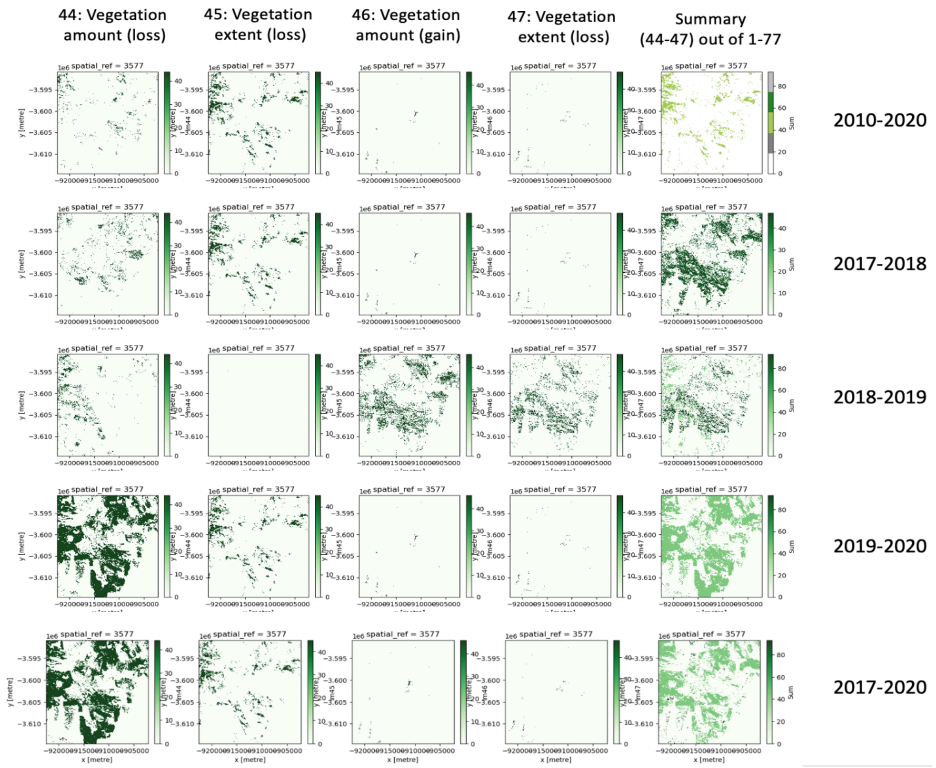

Figure 5-8: Impact maps generated for Mt. Ney, Western Australia of vegetation amount and extent loss and gains and summaries of these for 2010-2020, 2017-2018, 2018-2019 and 2020. Whilst these consider 4 impacts classes (numbered 44, 45, 46 and 47), up to 32 classes relevant to forest change can be included.

The use of global taxonomies (the FAO LCCS for land cover classification and the Global Change Taxonomy) and the Evidence-Based Change Framework for identifying change from accumulated evidence of impacts and pressures has relevance at local to global scales. Whilst national and continental mapping has been provided by Australia and Wales, there is a requirement for implementation at global level to support interpretation of the changes in AGB resulting from different impacts and the magnitudes and directions of AGB change in the CCI BIOMASS epochs. However, this currently requires reference to and comparison of existing land cover mapping for multiple years. Most of these products (e.g., ESA CCI land cover) are of relatively coarse spatial resolution (typically 300 m to 1 km) and have different legends that may be based on the FAO LCCS or other taxonomies. However, in most cases, these be deconstructed into environmental descriptors (OEDs and EEDs primarily) and then reconstructed to generate maps according to the FAO LCCS. Once achieved, evidence for impacts can be discerned, whilst pressures can be obtained by referencing a range of information obtained either from Earth observation data or other sources. More detailed application has already been obtained for Australia and Wales, and so these sites provide capacity to validate the interpretations of change at the global level. AGB data for multiple epochs can contribute to this evidence base, but the comparisons of land covers and the environmental descriptors used for their construction and description also allow better understanding of the nature of change; whether this is a slow or fast loss or gain that is complete or partial. The following sections provide more details on this proposed approach.

5.4. Global implementation of the evidence-based change framework.

5.4.1. Deconstruction and reconstruction of global land covers for multiple years.

CCI BIOMASS generates AGB datasets globally and for multiple epochs (2010 and annually from 2017 to 2020). Comparisons of these datasets can be **external** to but reference evidence for change impacts and pressures obtained through time series comparison of other independent environmental descriptors and/or land cover maps generated from these. Such an approach is particularly useful for interpreting rapid losses of AGB indicated by the stock-difference approach or slower decreases or increases suggested through use of the Mann-Kendall and/or Theil-Sen slope trend analysis, with consideration given to their respective uncertainties. The use of the AGB dataset can also be **internal** to the evidence-based change framework, providing additional information that can support or question the nature of change. Regardless as to whether the AGB datasets are used external to or internally within the evidence-based change framework, relevant continuous and categorical environmental descriptors need to be available for all forested regions of the World and represent time-periods that align with the CCI AGB estimates.

The *Living Earth* land cover and change maps, whilst developed within the globally applicable ODC have only been implemented for continental Australia (1985-2022) and nationally for Wales (2018-2022) using, respectively, the entire time series of Landsat and Sentinel-1/2 ARD data. Whilst these regions have provided demonstration of the approach, global implementation of *Living Earth* would require the transfer and testing of all retrieval/classification algorithms within big data platforms that house or give access to the full archive of satellite sensor data (Landsat and/or Sentinel-1 or -2) but also others, including ENVISAT ASAR, ALOS PALSAR and ALOS-2 PALSAR-2). If this could be achieved, there is potential to construct the land cover and change maps globally using the existing *Living Earth* software, but this is unlikely in the short term.

An alternative approach is to deconstruct existing global land cover maps into layers that each represent the OEDs and EEDs of the FAO LCCS and then reconstruct the maps according to this taxonomy. Initially, the maps can be deconstructed to form the FAO LCCS Level 3 categories, and then further descriptions provided using deconstructed categorical layers, with lifeform, leaf type and phenology being those relevant to vegetation AGB. However, categorical (e.g., Global Mangrove Watch mangrove extents) and continuous environmental descriptors external to these classifications can also be summarised and included, with notable examples being water hydroperiod (typically based on months of observed inundation), canopy cover (%) and canopy height (m). Where obtained, these can be used to increase the number of inputs and land cover classes generated. Once undertaken, Additional Environmental Descriptors, including AGB, can be integrated to further describe the land cover classes.

This approach has been evaluated and demonstrated as viable using a) the ESA CCI Land Cover 300 m spatial resolution and b) the High-Resolution Copernicus land covers 10 m resolution land cover products, with implementation undertaken at a global scale using Google Earth Engine (GEE). The ESA CCI Land Cover data for 2010, 2017, 2018, 2019 and 2020 gives a greater number of categories and hence have been ingested to GEE and deconstructed into selected component classes of the FAO LCCS, commencing with the OEDs (i.e. Level 3 (Table 1) and then the EEDs of lifeform, leaf type, phenology and water state).

Table 5-1: Look up table for translating the ESA CCI Land Cover classes to the FAO LCCS classes.

		FAO LCCS OED or EED[1]				
ESA Code	**ESA Label**	**Level 3**	**Acr.**	**Life form**	**Leaf type**	**Phen-ology**
0	No Data	0	ND			
10	Cropland, rainfed	111	CTV	H		
11	Herbaceous cover	111	CTV	H		
12	Tree or shrub cover	111	CTV	W		
20	Cropland, irrigated or post-flooding	123	CAV	H		
30	Mosaic cropland (>50%) / natural vegetation (tree, shrub, herbaceous cover) (<50%)	111	CTV	W		
40	Mosaic natural vegetation (tree, shrub, herbaceous cover) (>50%) / cropland (<50%)	112	NTV	H		
50	Tree cover, broadleaved, evergreen, closed to open (>15%)	112	NTV	W	B	E
60	Tree cover, broadleaved, deciduous, closed to open (>15%)	112	NTV	W	B	D
61	Tree cover, broadleaved, deciduous, closed (>40%)	112	NTV	W	B	D
62	Tree cover, broadleaved, deciduous, open (15-40%)	112	NTV	W	B	D
70	Tree cover, needleleaved, evergreen, closed to open (>15%)	112	NTV	W	N	E
71	Tree cover, needleleaved, evergreen, closed (>40%)	112	NTV	W	N	E
72	Tree cover, needleleaved, evergreen, open (15-40%)	112	NTV	W	N	E
80	Tree cover, needleleaved, deciduous, closed to open (>15%)	112	NTV	W	N	D
81	Tree cover, needleleaved, deciduous, closed (>40%)	112	NTV	W	N	D
82	Tree cover, needleleaved, deciduous, open (15-40%)	112	NTV	W	N	D
90	Tree cover, mixed leaf type (broadleaved and needleleaved)	112	NTV	W		
100	Mosaic tree and shrub (>50%) / herbaceous cover (<50%)	112	NTV	W		
110	Mosaic herbaceous cover (>50%) / tree and shrub (<50%)	112	NTV	H		
120	Shrubland	112	NTV	W		
121	Evergreen shrubland	112	NTV	W		E
122	Deciduous shrubland	112	NTV	W		D
130	Grassland	112	NTV	H		
140	Lichens and mosses	112	NTV	H		
150	Sparse vegetation (tree, shrub, herbaceous cover) (<15%)	112	NTV	W		
151	Sparse tree (<15%)	112	NTV	W		
152	Sparse shrub (<15%)	112	NTV	W		
153	Sparse herbaceous cover (<15%)	112	NTV	H		
160	Tree cover, flooded, fresh or brackish water	124	NAV	W		
170	Tree cover, flooded, saline water	124	NAV	W		
180	Shrub/herbaceous cover, flooded, fresh/saline/brackish water	124	NAV	H		
190	Urban areas	215	AS			
200	Bare areas	216	BS			
201	Consolidated bare areas	216	BS			
202	Unconsolidated bare areas	216	BS			
210	Water bodies	220	WAT			
220	Permanent snow and ice	220	WAT			

[1]CTV=Cultivated/Managed Terrestrial Vegetation, NTV=Natural/Semi-natural Terrestrial Vegetation, CAV=Cultivated/Managed Aquatic Vegetation, NAV=Natural Aquatic Vegetation, AS=Artificial Surface, BS=Naturally Bare Surface, WAT=water (natural or artificial); W=Woody (Numerical code=1), H=Herbaceous(2); B=Broadleaved (1), N=Needleleaved (2); E=Evergreen (1), D=Deciduous (2). Water is given a value of 1 whilst permanent snow and ice a value of 2 or 3, with this determined through reference to external layers (e.g., ESA CCI snow cover)

Further EEDs were obtained from other global datasets including water hydroperiod (Pekel et al., 2016) and canopy cover. These environmental descriptors have been reconstructed to generate global classifications of land cover according to the FAO LCCS for all years (see Figure 5-9 for OEDs and lifeform respectively). Further descriptions have been provided by referencing globally available AEDs including ESA CCI Biomass AGB datasets for each year (see Figure 5-10).

a)

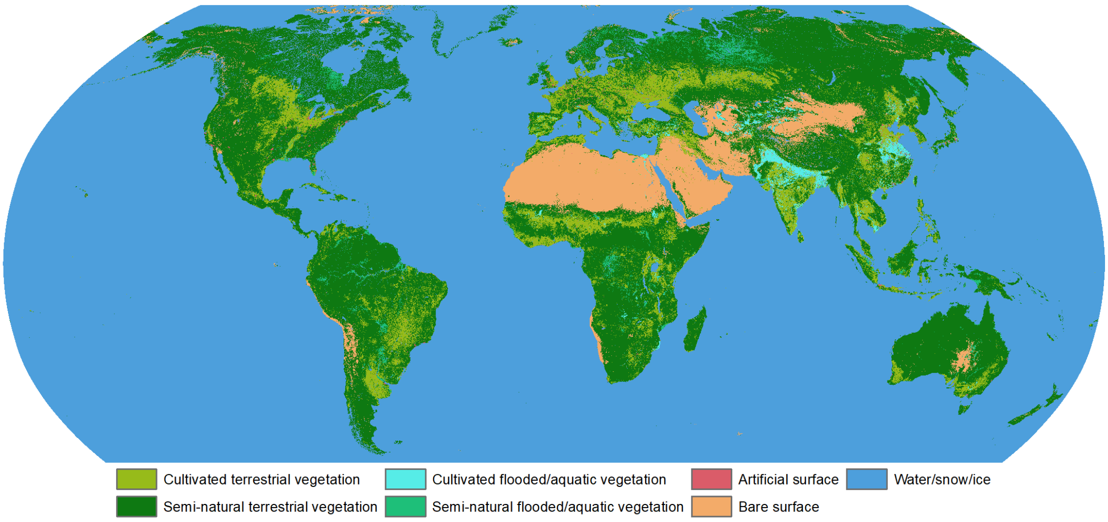

b)

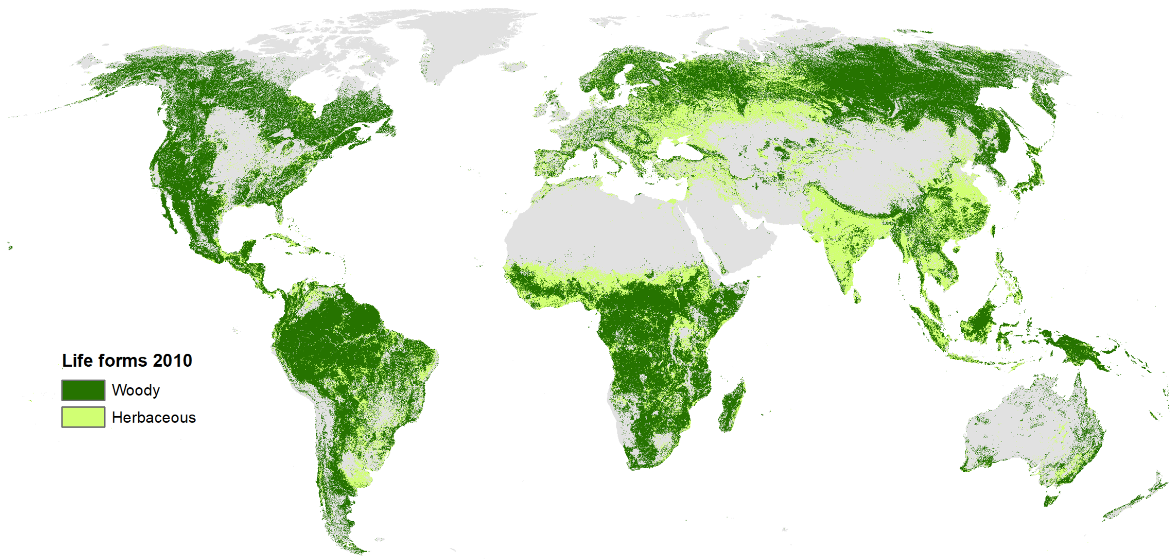

Figure 5-9: a) Global land cover map for 2010 with the FAO LCCS taxonomy, generated by deconstructing the ESA CCI 300 m resolution Land Cover product into seven classes defined in the third dichotomous phase (Level 3) of the taxonomy. b) More detailed global maps generated by integrating categorical environmental descriptors deconstructed and extracted from ESA CCI Land Cover (lifeform, leaf type, phenology, water type) and further described using actual or summaries of continuous environmental descriptors (e.g., canopy cover, water-hydroperiod). As existing global maps are

available for multiple years, multiple deconstructions and reconstructions into the FAO LCCS was undertaken, with this facilitating the detection of change impacts listed in the Global Change Taxonomy.

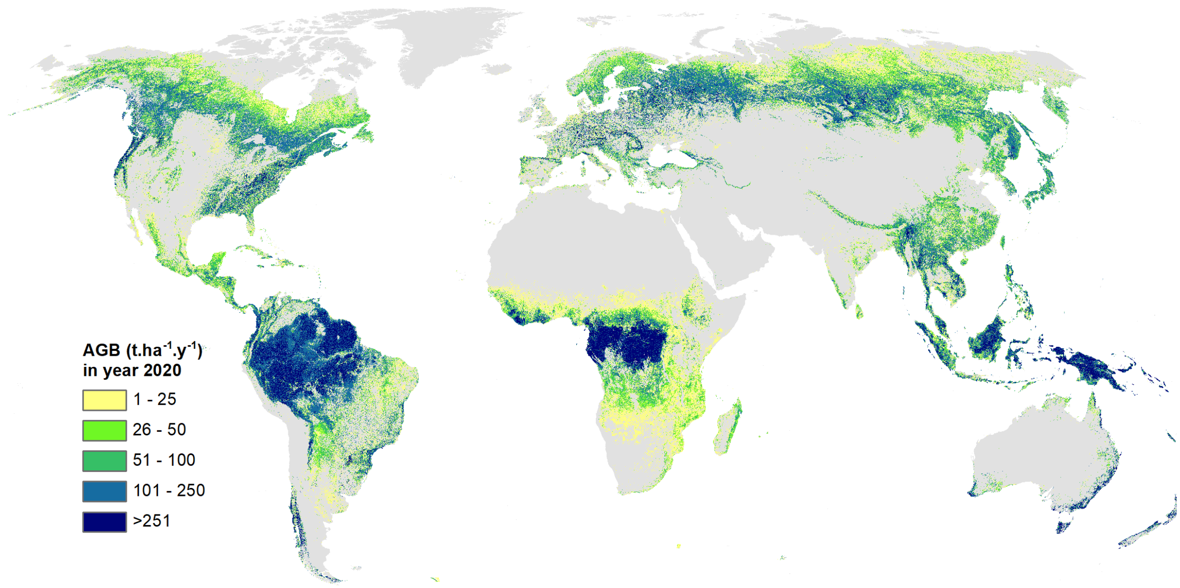

Figure 5-10: Global ESA AGB map for year 2020.

5.4.2. Implementation of the evidence-based change framework

Following generation of the global land cover maps according to the FAO LCCS, the detection and mapping of change impacts from evidence can then be achieved by comparing these and the contributory environmental descriptors between time-separated periods, in this case 2010-2020 and annually from 2017 to 2020. This comparison can be augmented by including the global ESA CCI BIOMASS AGB estimates for these epochs and the assessment of change and associated uncertainty obtained using the stock difference and/or trend analysis methods.

The stock-based approach is best used to provide evidence of change when comparing AGB estimates from two time-separate periods (e.g., years, including 2010-2020) whilst the trend analysis method can be used when time series of AGB data are available. Whilst this approach is best applied when comparing AGB estimates for 2017, 2018, 2019 and 2020, comparisons can also be made with 2010 with two main caveats; first, these estimates may differ in part because of the use of different sensors in their generation and hence establishing trends may be compromised and, second, significant change might have occurred in the intervening period. Demonstration that both methods can be applied globally is provided in Figure 5-11 and Figure 5-12, which show respectively the generation of a stock-difference map between 2017 and 2020 and a Theil-Sen slope estimator map giving the direction and magnitude of AGB change determined using annual AGB estimates for 2017 to 2020. These associated assessments of uncertainty can be integrated within the evidence-based change approach to establish where change has occurred and give confidence in the detection, but also interpretation of the causes and consequences of change (e.g., complete or partial loss or gain of AGB because of changes in land cover extent (conversions) or increases/decreases in AGB as a result of modification of the vegetated landscape). The evidence-based change approach can support (quantitatively and qualitatively), the interpretation of the change as well as its direction and magnitude. This can be assisted by other continuous layers that align with AGB, such as canopy cover and density and height as well as indices (e.g., the Normalised Difference Vegetation Index (NDVI) or fractional covers (photosynthetic, non-photosynthetic and/or bare)). In many cases, as demonstrated using the DEA which houses the entire archive of Landsat and also Sentinel-2 data, these metrics can be generated on a sub-annual (e.g., weekly to monthly basis). Other estimates of AGB that are available more frequently and for longer periods of time (e.g. those based on L-VOD or C-band scatterometers) can also be integrated.

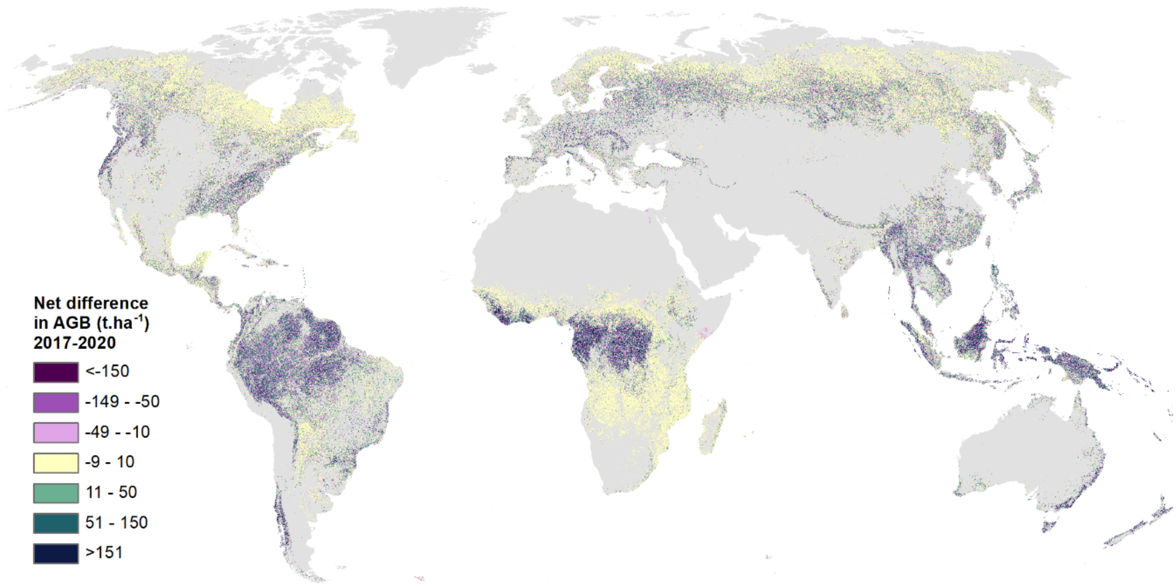

Figure 5-11: Net difference in ESA CCI AGB between 2017 and 2020, averaged to a 10 x 10 km grid cell, with no change pixels ignored. No forest mask applied.

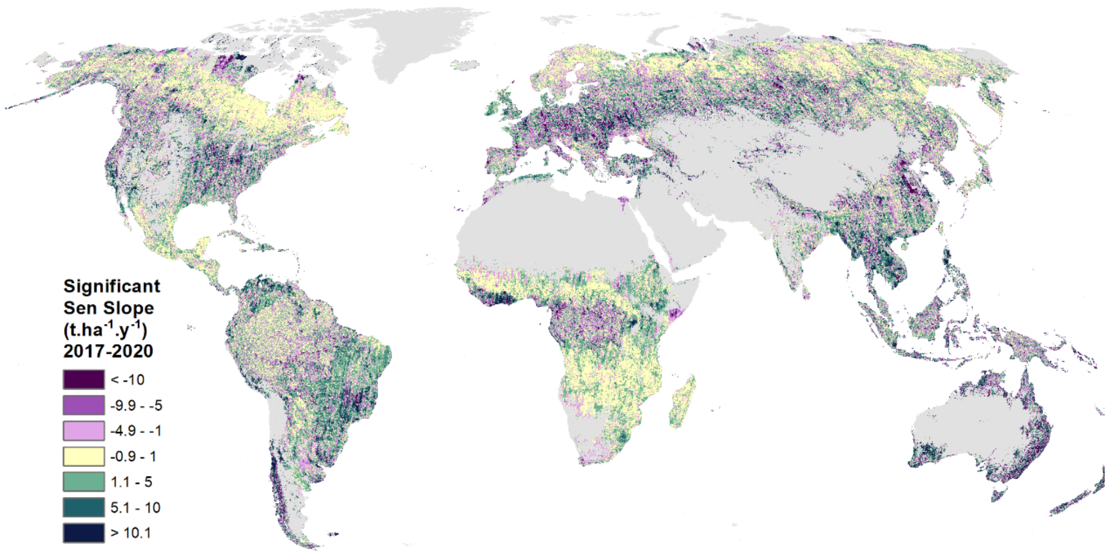

a)

b)

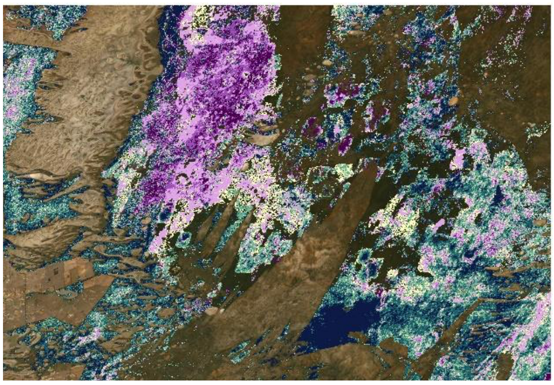

c)

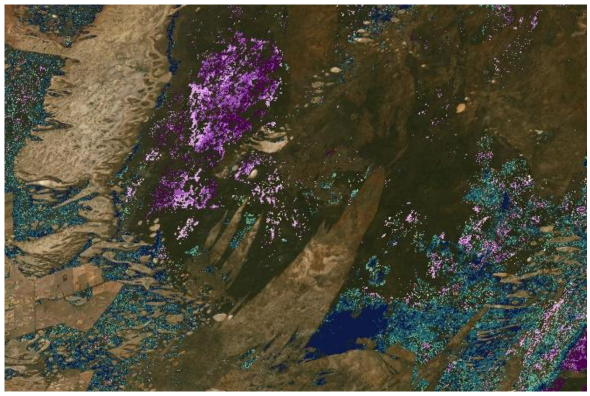

Figure 5-12: a) Global annual change in ESA CCI BIOMASS AGB based on the Theil-Sen slope estimator between 2017-2020, averaged to a 10 x 10 km grid cell, with no change pixels ignored. No forest mask applied. b and c) Example of areas experiencing burning near Mt Ney in Western Australia: b) shows slope values of AGB change at 100 m spatial resolution, regardless of trend significance, while c) shows slope values associated with significant trends only (colour legend provided in a).

Information on pressures driving change is obtained from a range of other sources that can identify the natural events or processes or human activities that alter the states and dynamics of forests. The sources of these data include many ESA CCI products, such as snow cover, fire, sea level and land surface temperature, and these are being explored.

5.5. Discussion

5.5.1. Stock-difference

The stock-difference approach (with associated quality flags) is a viable method for a) providing uncertainty in quantified differences in AGB between successive dates and b) giving a degree of confidence (i.e., reliable, potential, or improbable) that changes detected are associated with a loss or gain of AGB. The success in applying the stock-difference approach is dependent on a) the periods (epochs) being compared and b) the rates, magnitudes, directions, and persistence of change. In ESA CCI BIOMASS, AGB estimates are compared over one decade (2010 and 2020) and annually from 2017 to 2020. Key considerations are:

a) The stock-difference approach performs best where forest loss is complete, rapid and persistent (i.e., remains as non-forest over the year or decade). In these situations, the estimated AGB of the forest prior to removal gives an estimate of the magnitude of the loss, subject to the uncertainty in this estimate prior to the change event.
b) Where partial removal of vegetation occurs, the reliability of detection depends on the AGB prior to the change, which varies with the setting (e.g., climate, slope, aspect, prior land management) within biomes, the proportional loss of AGB, and the uncertainty in AGB estimation prior to and following the AGB change.
c) Detecting partial losses of AGB over time will further depend upon the amount accumulated by forests following the change (through growth) over the period of comparison (decades or years) and the associated uncertainty of the pre- and post-change AGB. Where forest loss is partial but has recovered, changes in AGB might be overlooked, particularly where estimates are a decade apart.
d) Gains in AGB are generally most rapid during the early stages of growth (e.g., on land recently cleared of natural forests or fully/partially harvested for timber and then replanted) but are unlikely to be detected when AGB estimates are compared between consecutive years, particularly given the often-high levels of uncertainty in the estimates. The exception is where forests are rapidly growing, as is often the case for commercial plantations and natural regenerating forests in productive regions (e.g., the tropics).
e) Gains and losses can take place over varying time series and may not be monotonic, particularly in highly dynamic environments (e.g., wooded savannas with a high frequency of fire events).

5.5.2. Mann-Kendall and Theil-Sen Slope Trend Analysis

The Mann-Kendall and Theil-Sen slope methods are best applied where AGB estimates are available for consecutive years, as is the case for 2017, 2018, 2019 and 2020. Whilst the CCI Biomass 2010 AGB data can be integrated, the use of different C- and L-band sensors in their generation can be misleading, partly as these differed between epochs (i.e., ALOS PALSAR and ENVISAR ASAR for 2010 and ALOS-2 PALSAR-2 and Sentinel-1 SAR for 2017-2020). A time series of AGB estimates that are more frequently generated and obtained using the same sensor types and operating modes is preferred, but this is often difficult to achieve. Another option is to consider and benchmark AGB trends with those obtained from time series of AGB estimates from other sensors (e.g., L-VOD, C-band scatterometers) or extrapolated from *in situ* measurements (e.g., with the Plot2Map tool) under the assumption that such trends correspond to reality. However, in the latter case, obtaining sufficient data from spatial locations and time-steps that facilitate this approach has proved problematic. Reference to time series of other metrics (e.g., Landsat-derived fractional cover of vegetation or spectral indices) can also indicate the nature of change (e.g., directions, magnitudes).

5.5.3. Evidence-based change

Whilst the stock-difference and trend analysis can be used stand-alone, there are considerable merits in including these within the evidence-based change framework developed through *Living Earth* that considers both change impacts and pressures and uses globally applicable land cover and change taxonomies. The accumulation of evidence from a diverse range of environmental descriptors and the land cover classes generated from these provides significant new potential to consistently describe the natural events and human activities leading to changes in AGB and whether these are complete (e.g., as established by an extent change of broad land covers, i.e., a conversion) or partial (a modification, indicated by a change in type, such as a predominantly woody to herbaceous lifeform or *vice versa*, or in amount – such as canopy cover or height). AGB estimates obtained from multiple epochs can also contribute evidence for change.

The generation of land cover maps for multiple years and integration of the stock-difference and trend analyses in DEA and the WDC has been demonstrated, with this allowing local evaluation for any area in Australia and Wales. However, within Phase 2 - Year 2 of CCI Biomass, these approaches have been implemented within GEE and global application has been demonstrated. The capacity to undertake an evidence-based approach has been enabled at a global level by a) deconstructing the legends of global land cover maps into individual environmental descriptors and then reconstructing these into the FAO LCCS taxonomy and b) including other environmental descriptors, including canopy density and water hyperperiod that are often of higher spatial resolution.

As existing land cover maps and environmental descriptors are available for multiple years, these can provide evidence for impacts and be used alongside spatial datasets representing the pressures driving change (e.g., bushfires, drought, storms, sea level fluctuation and flooding), including those that take place simultaneously or sequentially. There is also capacity to discern these pressures directly from the time series of land covers and environmental descriptors, with notable examples being the age of forests and frequency of burning and water inundation obtained from time series or the use of context, geographical location, or shape metrics (e.g., to differentiate fire scars from clear cuts or shifting agriculture).

A limitation of the approach is that the current mapping of land covers globally is based on the deconstruction and reconstruction of the ESA CCI land cover maps at 300 m spatial resolution, even though this can be augmented by EEDs such as canopy cover and water hydroperiod and the classes can be further described using, for example, AGB. Several of the ESA CCI land cover classes are ambiguous (e.g., in differentiating between woody and herbaceous vegetation) and so further refinement is needed. However, there are considerable opportunities to achieve this refinement by including an increasing number of existing datasets, with examples being the Global Mangrove Watch mangrove extent layers and canopy height estimates based on the GEDI and ICESAT-2 lidar datasets.

6. Conclusions

The development of the CORE retrieval algorithm of the CCI Biomass project has implemented several aspects presented in the previous versions of this document. The current CORE algorithm has reached maturity, in the sense that it can be applied to generate AGB maps for any year provided that the set of radar backscatter measurements are available. However, this does not imply that the AGB estimates are free from errors, given that the retrieval relies on observations that only see a portion of the forest biomass (above ground) and the inversion models implement several assumptions that tend to generalize the response of the radar backscatter to AGB.

We see two major developments that may further improve the accuracy of the retrieval, beyond the improvements already achieved in the first five years of the CCI Biomass project:

- Consolidation of LiDAR observations in the CORE retrieval algorithm.
- Integration of coarse resolution and high resolution EO datasets

The former will provide a more solid baseline for the models implemented in the retrieval model. The latter will increase the reliability of the AGB estimates in time and improve the accuracy of the AGB estimates in forests with the highest AGB densities (> 300 Mg ha^{-1}).

Although not directly used in the retrieval algorithms, plot inventory measurements have a fundamental role in characterising spatial errors in AGB estimates by modelling biases. The modelling of biases was prototyped but needs further development.

The two methods currently considered for identifying and qualifying changes in AGB in CCI BIOMASS are the stock-difference and trend-analysis approaches, with both applied at a global level through GEE.

The stock-difference approach has already been demonstrated globally. ESA Biomass AGB per-pixel (100 m) estimates for 2010, 2017, 2018, 2019 and 2020 and associated standard deviations have been generated and the standard deviation of the stock-difference method has been provided in the ESA product for the 2017-2018, 2018-2019 and 2019-2020 differences. Per-pixel quality flags have also been generated according to whether the histograms associated with the pixel at the two epochs are disjoint or fully or partially overlapping and can be used to interpret the reliability of the difference detected by pixel.

The Mann-Kendall and Theil-Sen slope have been used to estimate trends, with the former determining the presence (or otherwise) of a trend and its significance over the selected time period and the Theil-Sen slope establishing the direction and magnitude of the trend. This approach is best applied to the annual time series of AGB estimates from 2017 to 2020 but can also be considered for use with all available estimates (i.e., 2010 to 2020). In this latter case, we need to consider the effects of both differences in sensor types used in the AGB estimation and changes in AGB that might have occurred during periods of no observation by satellites.

The integration of AGB estimates within an evidence-based change framework presents significant benefits in terms of understanding and confirming (or otherwise) changes in AGB as a result of conversions or modifications of land covers. The impacts of these are diverse and result from a range of natural events and processes (abiotic and biotic) and human activities with these driven by diverse pressures. Following regional/country level demonstration in Australia and Wales, the research undertaken in this year, CCI BIOMASS has attained capacity to implement the evidence-based change framework developed through Living Earth globally within GEE. This has been achieved by deconstructing existing mapping (primarily the ESA CCI Biomass 300 m land cover) into its component EDs and then reconstructing the maps according to the FAO LCCS using these and other descriptors such as canopy density with further descriptions provided by including the ESA CCI AGB estimates. Associated estimates of uncertainty can also be integrated to inform the evidence for change and the reliability of the AGB estimates and change comparisons. From now on, these maps can be continually improved in content, spatial resolution and the temporal frequency of generation.

Whilst the use of the stock-difference and trend analyses approaches within an evidence-based framework has been adopted as the best current approach for identifying and assessing the reliability of AGB change, other methods continue to be explored. The validation of maps of AGB change is also being undertaken with reference to *in situ* data and very-high resolution Earth observation data (including airborne LIDAR and Planetscope), as outlined in the Product Validation Plan.

7. References

Araza, A., de Bruin, S., Herold, M., Quegan, S., Labriere, N., Rodriguez-Veiga, P., Avitabile, V., Santoro, M., Mitchard, E.T.A., Ryan, C.M., Phillips, O.L., Willcock, S., Verbeeck, H., Carreiras, J., Hein, L., Schelhaas, M.-J., Pacheco-Pascagaza, A.M., da Conceição Bispo, P., Laurin, G.V., Vieilledent, G., Slik, F., Wijaya, A., Lewis, S.L., Morel, A., Liang, J., Sukhdeo, H., Schepaschenko, D., Cavlovic, J., Gilani, H., Lucas, R., 2022. A comprehensive framework for assessing the accuracy and uncertainty of global above-ground biomass maps. *Remote Sensing of Environment* 272, 112917. https://doi.org/10.1016/j.rse.2022.112917

Carreiras, J.M.B., Quegan, S., Le Toan, T., Ho Tong Minh, D., Saatchi, S.S., Carvalhais, N., Reichstein, M., Scipal, K., (2017). Coverage of high biomass forests by the ESA BIOMASS mission under defense restrictions. *Remote Sensing of Environment* 196, 154–162. https://doi.org/10.1016/j.rse.2017.05.003

Clinton, N. (2020) Non-Parametric Trend Analysis. Google Earth Engine developer community tutorials. https://developers.google.com/earth-engine/tutorials/community/nonparametric-trends

Di Gregorio, A. (2005). Land cover classification system: classification concepts and user manual: LCCS (Vol. 2). Food & Agriculture Organization.

Dubayah, R., Blair, J.B., Goetz, S., Fatoyinbo, L., Hansen, M., Healey, S., Hofton, M., Hurtt, G., Kellner, J., Luthcke, S., Armston, J., Tang, H., Duncanson, L., Hancock, S., Jantz, P., Marselis, S., Patterson, P., Qi, W., Silva, C., (2020). The Global Ecosystem Dynamics Investigation: High-resolution laser ranging of the Earth's forests and topography. *Science of Remote Sensing* 100002. https://doi.org/10.1016/j.srs.2020.100002

Farr, T., Rosen, P. A., Caro, E., Crippen, R., Duren, R., Hensley, S., Kobrick, M., Paller, M., Rodriguez, E., Roth, L., Seal, D., Shaffer, S., Shimada, J., Umland, J., Werner, M., Oskin, M., Burbank, D. and Alsdorf, D. (2007). The Shuttle Radar Topography Mission. *Review of Geophysics,* 45 (RG2004), 1-33.

Gilbert, R.O. (1987). Statistical Methods for Environmental Pollution Monitoring, Wiley, NY.

Kay, H., Santoro, M., Cartus, O., Bunting, P., Lucas, R.,(2021). Exploring the relationship between Forest Canopy Height and Canopy Density from spaceborne LiDAR Observations. Remote Sensing 13, 4961. https://doi.org/10.3390/rs13244961.

Kendall, M. G. (1938). A new measure of rank correlation. *Biometrika* 39: 89–93

Kendall, M.G. (1975). Rank Correlation Methods, 4th edition, Charles Griffin, London.

Krieger, G., Moreira, A., Fiedler, H., Hajnsek, I., Werner, M., Younis, M. and Zink, M. (2007). TanDEM-X: a satellite formation for high-resolution SAR interferometry. *IEEE Transactions on Geoscience and Remote Sensing,* 45 (11), 3317-3341.

Lucas, R. M., S. German, G. Metternicht, R. K. Schmidt, C. J. Owers, S. M. Prober, A. Richards, et al. 2022. "A Globally Relevant Change Taxonomy and Evidence-Based Change Framework for Land Monitoring." Global Change Biology, 1–25. doi:10.1111/gcb.16346.

Mann, H. B. (1945). Nonparametric tests against trend. *Econometrica* 13: 245–259.

Mann, H. B., and D. R. Whitney. (1947). On a Test of Whether one of Two Random Variables is Stochastically Larger than the Other. The Annals of Mathematical Statistics 18: 50–60.

Neuenschwander, A. and Pitts, K. (2019). The ATL08 land and vegetation product for the ICESat-2 Mission. *Remote Sensing of Environment,* 221, 247-259.

Oesterwind, D., Rau, A., & Zaiko, A. (2016). Drivers and pressures – Untangling the terms commonly used in marine science and policy. Journal of Environmental Management, 181, 8–15. https://doi.org/10.1016/j.jenvman.2016.05.058

Planque, C., Punalekar, S., Lucas, R., Chognard, S., Owers, C. J., Clewley, D., Bunting, P., Sykes, H., & Horton, C. (2020). Living Wales: Automatic and routine environmental monitoring using multi-source earth observation data. In K. Schulz, U. Michel, & K. G. Nikolakopoulos (Eds.), Earth resources and environmental remote sensing/GIS applications XI, 115340C, Proceedings of SPIE - The International Society for Optical Engineering (Vol. 11534). SPIE, Earth Resources and Environmental Remote Sensing/GIS Applications XI 2020, Virtual, Online, United Kingdom of Great Britain and Northern Ireland, 21 Sep 2020. https://doi.org/10.1117/12.2573763

Punalekar, S. M., C. Planque, R. M. Lucas, D. Evans, V. Correia, C. J. Owers, P. Poslajko, P. Bunting, and S. Chognard. 2021. "National Scale Mapping of Larch Plantations for Wales Using the Sentinel-2 Data Archive." Forest Ecology and Management 501: 119679. doi:10.1016/j.foreco.2021.119679.Quegan, S., Le Toan, T., Chave, J., Dall, J., Exbrayat, J.-F., Minh, D.H.T., Lomas, M., D'Alessandro, M.M., Paillou, P., Papathanassiou, K., Rocca, F., Saatchi, S., Scipal, K., Shugart, H., Smallman, T.L., Soja, M.J., Tebaldini, S., Ulander, L., Villard, L., Williams, M., (2019). The European Space Agency BIOMASS mission: Measuring forest above-ground biomass from space. *Remote Sensing of Environment* 227, 44–60. https://doi.org/10.1016/j.rse.2019.03.032

Santoro, M. and Cartus, O. (2018). Research pathways of forest above-ground biomass estimation based on SAR backscatter and interferometric SAR observations. *Remote Sensing,* 10 (4), 608, doi:10.3390/rs10040608.

Sen, P. K. (1968). Estimates of the regression coefficient based on Kendall's tau. *Journal of the American Statistical Association.* 63: 1379–1389.

Theil, H. (1950). A rank-invariant method of linear and polynomial regression analysis I, II and III. In *Proceedings of the Section of Sciences, Koninklijke Academie van Wetenschappen te,* (Amsterdam), 386–92.

Walker, W. S., Kellndorfer, J. M., LaPoint, E., Hoppus, M. and Westfall, J. (2007). An empirical InSAR-optical fusion approach to mapping vegetation canopy height. *Remote Sensing of Environment,* 109 (4), 482-499.